ENERGY ABSORPTION PERFORMANCE OF PRESS-FORMED SHELL

プレス成形シェルのエネルギー吸収特性

by
ZUBAIR BIN KHALIL

A Thesis Submitted to the
Graduate School of Engineering, Gifu University
as a Partial Fulfillment of the
Requirements for the degree of
DOCTOR OF ENGINEERING
(March 2016)

Supervisor:
Prof. Dr. Minoru Yamashita

CONTENTS

Acknowledgement i

Summary ii

Chapter 1: Introduction 1

1.1 Background and Objectives 1
1.2 Contents of thesis 5

Chapter 2: Deformation Behavior of Press Formed Shell by Indentation and Its Numerical Simulation (Hindawi Publishing, Journal of Engineering, Vol. 2015 (2015), Article ID 453931) [34] 6

2.1 Introduction 6
2.2 Test material and experimental conditions 6
2.3 Experimental results and discussions 10
2.4 Numerical simulation 15
2.4.1 Computational conditions 15
2.4.2 Computational results and discussions 18
2.5 Conclusions 25

Chapter 3: Energy Absorption Performance of Press-Formed Shell under Impact (Elsevier, Procedia Engineering, Vol. 81(2014), pp. 951-956) [35] ... 26

3.1 Introduction 26
3.2 Test material and experimental procedure 26
3.3 Experimental results and discussions. 32
3.4 Energy performance evaluation 43
3.5 Conclusions 47

Chapter 4: General Conclusions 48

References 50

Acknowledgement

In the name of Allah, the Most Gracious and the Most Merciful

I praise and thank to God for making it possible for me to graduate from a doctorate course at Gifu University, Japan, and for granting me the prosperity to work on a research field that I have been working on throughout my academic years. Thank you God for giving me the strength and perseverence in achieving my goal.

I would like to extend my appreciation and gratitude to every person who has in one way or another contributed in making this research possible.

First of all, I would like to express my deepest appreciation and gratitude to my main supervisor, Professor Dr. Minoru Yamashita. You have been a tremendous mentor for me. I would like to thank you for encouraging me throughout my research and guiding me to become a research scientist. Without your patience, support and guidance, it would be difficult for me to go through the research process. Your advice on both my research as well as on my social life have been priceless. I am honoured to have such a generous concerned and thoughtful doctoral advisor.

I would also like to extend my gratitude to my co-supervisor, Professor Dr. Toshio Hattori. All your advice and opinions have been a great help to break through the hurdles in my research.

Special thanks to my family for their love and flowing encouragement throughout these years. Words cannot express how grateful I am to my father, my mother, my mother-in law, and father-in law for all the sacrifices that all of you have made on my behalf. Your prayers for me have helped me go through the difficult times. I am also very grateful and indebted to my beloved wife Mrs. Nurul Izwani Binti Mustapa who has spent sleepless nights with me and always supported me through her unconditional love. I would like to extend my special appreciation to my beloved kid, Adam Harith for always cheering my life, making me smile, and for understanding my predicaments during those weekends when I have to spend time on this present work instead of playing with you. Words cannot express my feelings nor my thanks for everybody's help.

I would also like to thank all of my friends who have supported me in this writing, and encouraged me to strive towards my goal. A big thank you to Mr. Tatsuya Tezuka, Mr. Yusuke Kuno, and Mr. Shuntaro Suzuki for not giving up doing our experiments together through the years in order to provide precise data. Thank you to all my colleagues in Yamashita Laboratory (previously known as Hattori Lab.) for sharing thoughts and supporting me throughout these years.

Last but not least, I am very thankful to the Malaysian Government in general and the Ministry of Education Malaysia (previously Ministry of Higher Education Malaysia) and Universiti Malaysia Pahang for providing financial support for this work to succeed.

Summary

Automobile body usually comprises many sheet metal components. Most of them are usually fabricated by various press-forming operations from sheet metal. The body designers will consider not only the strength for durability but also the structural ability to protect the occupants during impact in a collision event. Sheet metal components are collapsible and this plays an important role as the shock absorber of the kinetic energy exploit plastic deformation. Shape and material of each part and the loading condition, etc. affect the deformation behavior at collision. Thus the main objective of this thesis is to obtain the basic information in constructing the guidelines when designing energy absorber.This is done by studying several simple conditions in energy absorbing deformation behavior.

In the thesis, two kinds of dome shaped shells made by press-forming were deformed by indentation of the simple shaped indentors. Effects on the shell shape, height and the indentor shape in the deformation behavior were then investigated. The objective is to show the fundamental effective information for crashworthy design of press-formed sheet metal parts. The dome shaped specimen was flat-top or hemispherical axisymmetric shell. This was produced by press-forming operation using a circular blank of aluminum alloy A5052. The head shape of the indentor was flat or hemispherical. Numerical simulation was also conducted to predict the deformation patterns and the forces in the press-forming and the indentation using the dynamic explicit finite element code DYNA3D (Public domain version). The energy absorption performance of the shell was evaluated as the consumed energy by the deformation where the indentor travelled up to the length equal to the shell height. The most effective deformation condition for such performance was obtained in the deformation of flat-top shell by flat-headed indentor. Rising tendency in indentation force was duller, when the hemispherical-headed indentor was applied, in contrast to the case where a flat-headed indentor was used. A peculiar crushing load characteristic was observed, when the load was increased, and then decreased for the combination of hemispherical shell and flat-headed indentor. Plastic buckling occurred due to the radial compressive stress upon the material contact to the flat part of the indentor. These phenomena were successfully reproduced in the numerical simulation. Further, when the Bauschinger effect of the material was appropriately introduced into the numerical simulation, the indentation force became closer to the experimental result.

In addition, experiment was also conducted on mild steel SPCE sheets using flat or hemispherical headed indentor under impact condition using a drop hammer or quasi-static one. As a result, several characteristic force variations appeared. Almost flat indentation force is available in the combination of hemispherical shell and round headed indentor. The in-plane compressive stress field in the material induces the increase in indentation force, which in turn increases the energy absorption capacity. The force in impact test of SPCE was approximately 1.5 times higher than that in quasi-static test. The experimental results obtained here implies that the strain-rate effect on the stress tends to be enhanced if the loading direction alters. On the other hand, when we compared the results to aluminium alloy A5052-H34, it did not show the same tendency as SPCE. Aluminum alloy A5052-H34 and mild steel SPCE have comparable performance in energy absorption under impact in the range of the present experiments. The positive strain-rate effect of SPCE under the reverse in loading direction may improve the performance. When comparing the energy absorption performance under impact for the 10 mm diameter indentor with the 30 mm one, the energy absorption performance of 10 mm indentor is around 20 % larger. The reason was because the concentrated indentation force by the indentor caused severe bending to the shell's wall, thus increasing the load to a higher level within the fracture limit of the shell height.

In the present study, several basic characteristics in the indentation behavior were revealed for the simple collapse conditions, thus providing some helpful guidelines in designing the collapsible parts and structures.

Chapter 1: Introduction

1.1 Background and Objectives

Automobile body usually consists of many sheet metal components. Most of them are usually fabricated by various press forming operations from sheet metal. They are often joined by resistance spot welding or other welding processes, bolt and nut, adhesives, etc. Automobile body designers consider not only the strength for durability but also structural ability to protect the occupants during impact by collision event. The acceptable limit in acceleration acting on the human body has to pass the satisfied level in the passive safety concept. Further, the cabin deformation by crash is also kept under a certain level. Sheet metal members are plastically collapsible to play the important role as shock absorber, which dissipates kinetic energy.

The body deformed by collision will crumple or buckle, resulting in complicated pattern because the plastic deformation in many components occurs at same time causing their mutual interaction inevitable. As seen in aircraft fuselage, helicopter body and train body, the energy absorbing structural design is also adopted for protection of occupants.

For several decades, increasing concerns have been paid in respect to the shock absorbing deformation of vehicle bodies. Impact absorber has many different types of shape, suitability, deformation patterns, destruction limit and impact absorbing ability range, whereby each one of their characteristic is suitable to each requirement and environment that is being used adequate to its own ability range. For example, in an internal part of a contena used for transporting high precision equipment, honeycomb structures impact absorber was adopted and similarly for vehicle, crush box such as cylindrical types are generally being used as its impact absorber. Especially, for honeycomb structures type, it is a stable and more efficient impact absorber with high mechanical strength and rigidity. So, it is considered the best structures available as impact absorbers and thus this structure is being used and applied at many places. However, such complex structures of honeycomb or cylindrical, will cost a much higher manufacturing cost and that by itself would be a problem. For airplanes, and space shuttle's landing equipment, and container's impact absorber part to prevent damage to goods, there is a need to install an impact absorber that had high impact absorbing ability, simple structure and lowest manufacturing cost are an essential factors. In additional, when safety first is a concern, disposable impact absorbers which could be easily replaced with a new one when needed are a must.

Furthermore, here in Japan, a country that is actively pursuing to become a recycling society, recyclability will also be considered into the design. Facing problems such as weight saving and recyclability, we would consider a material that possesses a specific strength higher than iron or steel and at the same time having higher recyclability. For this purpose, aluminium alloy is the most effective material. Similarly, the number one contributor to global warming effect, CO_2 due to green house effect gas problem should also be considered at the same time. So, parts of the strategy to be considered into the design of the vehicle and its parts is the weight saving design.

Several papers discussing the collapse deformation have been published, and they cover a wide range of thin-walled structures, e.g., circular or square tubes, frusta, struts, honeycombs by Alghamdi [1, 2] and Olabi et al [3]. In an experimental study on frusta, El-Sobky[4] reported that a top constrained frusta exhibited highest increment in the magnitude of specific energy absorption capacity than full constrained, based or non-constrained one. It has also been found by Mohamed Sheriff [5] and Niknejad [6] that shell or frusta indentation load or energy absorption was influenced by the parameters like flow stress, thickness and angle. This also conforms to conclusions by Mamalis [7] which stated shell geometry is a significant factor affecting the deformation modes and the buckling loads for frusta. As a practical example, crush deformation of the helicopter subfloor structure assembled with sheet metal parts by riveting was studied for improvement of the energy absorption capability by Bisagni[8]. Furthermore, constitutive modeling for prediction of material failure was described for crashworthiness, where the shell element splitting techniques was demonstrated for crack propagation [9].

Yamashita et al. [10], Jones [11, 12] and Kim [13] summarized that thin-walled tubes made from both aluminum alloy and mild steel specimen which have different cross-sectional geometries tested under quasi-static and dynamics (with initial velocity, $V_0 \leq 20$ m/s) axial crushing forces, circular type tubes have the highest crush strength and was the most effectives energy absorbing structures than hexagonal, square, double hat and top hat accordingly. It is also anticipated that hexagonal with corner more than 11 have almost saturates crush strength and the one with less than six corners has a tendency to collapse before functioning as energy absorbers. Many factors can be raised such as the number of corners, wall thickness, cross-sectional area, diameter-to-thickness ratio, plastic hardening rate that will influence the specimen crush strength or energy absorbing effectiveness.

For the frontal crash safety of automobile, many investigations were performed for the collapse deformation of tubular structures. The deformation of tubular structures is sensitive for the geometries, dimensions and supporting condition, etc. Axial compressive deformation of circular and square steel tubes was theoretically well predicted [14]. Collapse of tubular structures with hat cross-section assembled with rivets, screws or/and adhesive were experimentally investigated [15]. The numerical model of hat tube was developed for the adhesive bonded one. The effect of the strength of the adhesive was demonstrated showing good agreement with the corresponding experiment [16]. An increase in flange width produces an increase in the mean loads and the axial displacement will increase stability while the longer tubular length was found to influence the collapse performance with the increase both the amount of energy absorbed and axial displacement before tendency for global buckling was reported by White [17].

Corbett [18] concludes that the energy absorbing capacity of mild steel tubes is strongly dependent on the rate of loading and hence the mass of projectile. For quasi-static, the ability of the tube to spread the load through indentation, crumpling and bending dictates the energy absorbing capacity of the tube depends on loading rate and material properties of the tube. At high rates of loading, the damage tends to be much localized regardless of the material properties of the tube and the energy

absorbing capacity of the tube that depends on factors such as projectile and tube inertia and rate effect.

Dome shaped or hemispherical shells were also the energy absorbers, where plastic collapse of aluminum egg-box panels subjected to out-of-plane compression was investigated by Zupana [19]. Collapse strength and energy absorption are sensitive to the level of in-plane constraint. The optimization of egg-box geometry was reported in the study conducted by Deshpande [20]. Aluminum shells with various radius / thickness ratios were compressed by two rigid plates under low speed condition. An analytical model was also proposed to predict the compressive load curve [21]. Spherical shells were crushed by a drop-hammer to investigate the energy absorption capacity. The numerical simulation was also performed. Their dynamic behavior was compared with that under quasi-static condition [22, 23].

Hemispherical metal domes were deformed by indenting several kinds of solid bars or tubes whose tip shape was flat, round headed or notched, etc. The effect of the indentation manner on the collapse load curve was examined both in experiment and finite element method by Shariati [24] and Dong [25]. For collapsible energy absorbers, inversion and reinversion deformations of frusta were found very appropriate, where the accumulated absorbed energy per unit mass and the usability of the absorber several times were considered by Alghamdi[2]. Honeycombs are also widely used as the shock absorbers. Impact experiment for various cell shapes and the corresponding numerical simulation were carried out by Yamashita [26].

From the problem stated above there is a need to search and study for a replacement of honeycomb structure, cylindrical structure and also the others and find a solution that have both wide range of absorbing ability and could be assemble into needed area as an impact absorbing parts. After some consideration and brainstroming, we have come up with an idea to make the most simple structure with an easy and feasible manufacturing process. The structure of our consideration is press-formed shell structure. This structure has already been widely used in mass production factory. So, if we could use the already existing equipment, and we could use the product's original properties with an additional property of impact absorber, not only we could save a lot of money, but we could also increase the safety measurement of the product.

The main objectives of this study is to obtain the basic information for constructing guidelines in designing the energy absorber by studying several simple conditions in energy absorbing deformation behavior. This study focus on simple axisymetric type structures that has been proven as stable and had the highest impact energy absorbing performance by our lab previous study on cylindrical structures. To achieve the study aim the following objectives has been considered for the research work :

1. To explore and study new type impact energy absorber that could be a replacement for the existing type structures that meet the least requirement of low manufacturing cost, weight saving design with wide range of impact absorbing ability.
2. To study the most suitable material that could match the design and needs of the above requirement.
3. Investigate each combinations impact energy absorption performance and their deformation behavior.

Based on all the information we have gathered, the present study will focus on the energy absorbing performance of press formed shell which has a very simple structure to fabricate, and can be installed as secondary energy absorber in all kinds of already existing structure either as additional shape or as filler. The shape of the press formed shell is flat top or hemispherical. The material was mild steel SPCE and aluminum alloy A5052-H34 sheet. Indentation was conducted using flat or hemispherical headed indentor under impact condition using a drop hammer or quasi-static one. In the study, shell shape and indentor's shape is varied. As mentioned in our objectives, there are several indentation force patterns which were observed from all the patterns we have studied as shown in example in Fig 1.1. So, it is very important for us to study and learn whether we could control the indentation force patterns to match the most suitable patterns for each case considered.

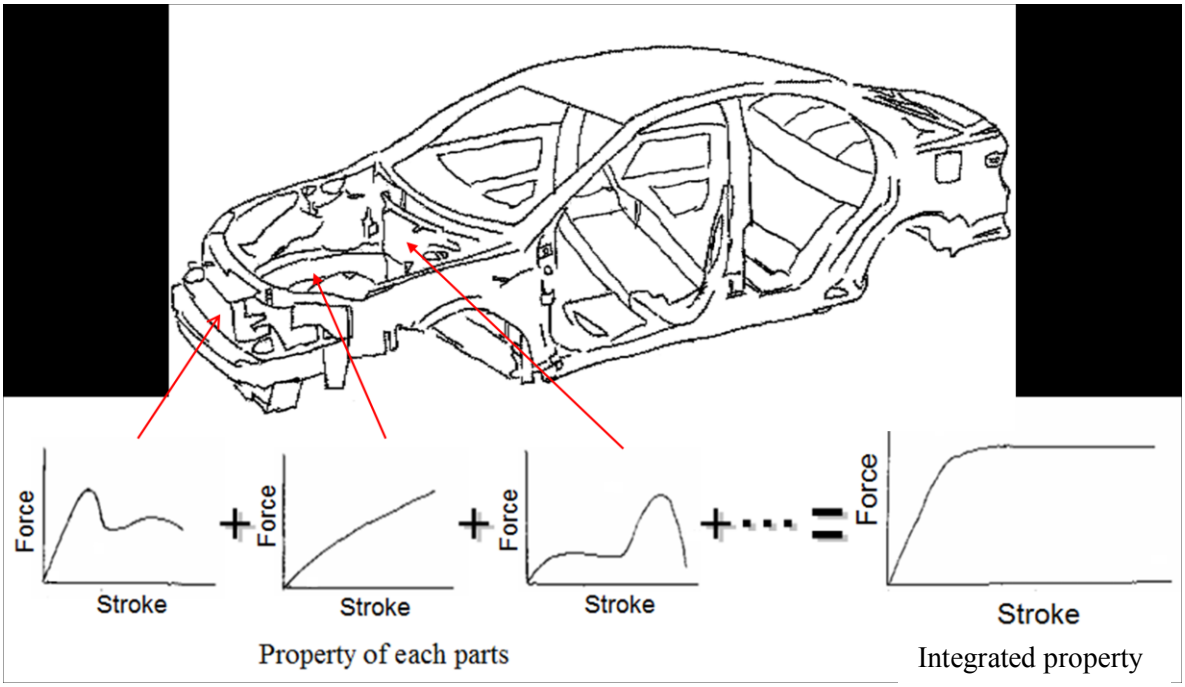

Fig 1.1 Properties of each part and its intergrated property

1.2 Contents of thesis

The thesis contains four chapters in total. Chapter 1 introduces the problem with the existing impact absorber and general remarks from the publication. Many types of impact absorber such as thin-walled structures, e.g., circular or square tubes, frusta, struts, honeycombs are already being used but problems such as manufacturing cost are the reason why we should consider a new type of impact energy absorber. Objectives of the present study are also included in this chapter.

In chapter 2, we will discuss a new type of impact absorber, which are fabricated by the press forming from aluminum alloy A5052-H34 sheet into flat top and hemispherical shells. They were deformed by the flat or hemispherical headed indentor. Deformation patterns and characteristic of the indentation force were investigated. Energy absorption performance in indentation deformation of the shells was estimated for indentation stroke corresponding to the shell height. Numerical simulation was also carried out by the dynamic explicit finite element method in order to present appropriate numerical model to achieve accurate prediction and the result was compared to the experimental result.

In chapter 3, higher deformation speed is applied to the deformation condition used in the previous chapter and we compare the results obtained in chapter 2. Further, mild steel SPCE shells are also tested. The energy absorption performance of each parameter was summarized from the viewpoint of the weight saving design. Influence on variance experimental parameter of indentor's shape and size on the energy absorbing performance of press formed shell was also conducted. The materials was aluminum alloy A5052-H34 sheets. Indentation using the flat or hemispherical headed indentor under impact condition was conducted with a drop hammer or quasi-static one. The results are then compared with the results of original indentor used in this study.

Lastly, chapter 4 summarizes the conclusions of all the chapters above. This summarization will be describing the findings of the study in the hope that this study will be the basis to obtain the basic information when constructing guidelines in designing the energy absorber and this is done by studying several simple conditions in energy absorbing deformation behavior.

Chapter 2: Deformation Behavior of Press-Formed Shell by Indentation and Its Numerical Simulation

(Hindawi Publishing, Journal of Engineering, Vol. 2015 (2015), Article ID 453931) [34]

2.1 Introduction

This study is focused on the energy absorbing performance of the press formed shell. The objective is to obtain the basic information in energy absorbing deformation behavior for optimizing the design of the collapsible components, e.g., in automobile and train bodies, building and structures. The shapes of the press formed shell are flat top and hemispherical. The material was aluminum alloy A5052-H34 sheet. Indentation was conducted using flat or hemispherical headed indentor. Numerical simulation was also carried out by the dynamic explicit finite element method in order to present appropriate numerical model to achieve accurate prediction.

2.2 Test material and experimental conditions

The test material is a commercially available aluminum alloy A5052-H34 sheet with 1 mm thickness. The mechanical properties are listed in Table 2.1. Specimens are the flat top and the hemispherical shells. They are formed from a circular blank with 80 mm diameter using a hydraulic type of 350 kN automated universal, Fig. 2.1, manufactured by Tokyo Testing Machine Incorporated and it is illustrated in Fig. 2.2.

Fig. 2.1 Hydraulic-type deep-drawing testing machine

The formed height was set to 10 mm. Forming operation was carried out under quasi-static condition, where the punch speed was about 0.1 mm/s. A commercially available lubricant (CD400, Daido chemical industry) for press forming was applied to all tool - material interfaces. The blank holding force was 3.5 kN which was the twice of the value calculated by Siebel's formula [27]. It gives the minimum blank holding force without flange wrinkling.

Details for Siebel's formula is explain as follow;

$$H = 0.0025\ \{(\beta - 1)^3 + 0.005\delta\} St \times A \times 2 \tag{2.1}$$

H : Blank force
D_0 : Blank diameter
d : Punch diameter
β : Drawing ratio (=D_0/d)
t_0 : Blank thickness
δ : Relative punch diameter (=d/t_0)
St : Ultimate Tensile Strength (U.T.S.)
A: Flange area

The tip shapes of the indentor are flat headed and hemispherical. The combinations of the shell and the indentor are shown in Fig. 2.3. The abbreviated notations FS, FF, SS and SF are used for the combinations. The first letter represents the shell shape, F: 'F'lat top or S: hemi'S'pherical shell. The latter represents the indentor, F: 'F'lat headed or S: hemi'S'pherical headed indentor. The indenting operation was also performed using the deep-drawing testing apparatus by substituting the indentor for the forming punch. The indentation speed was about 0.1 mm/s.

Table 2.1. Mechanical properties of test material.

Material	C (MPa)	n	U.T.S. (MPa)	E (%)
A5052-H34	383	0.15	248	8.3

Plastic property: $\sigma = C\varepsilon^n$, U.T.S.: Ultimate tensile strength, E: Total elongation

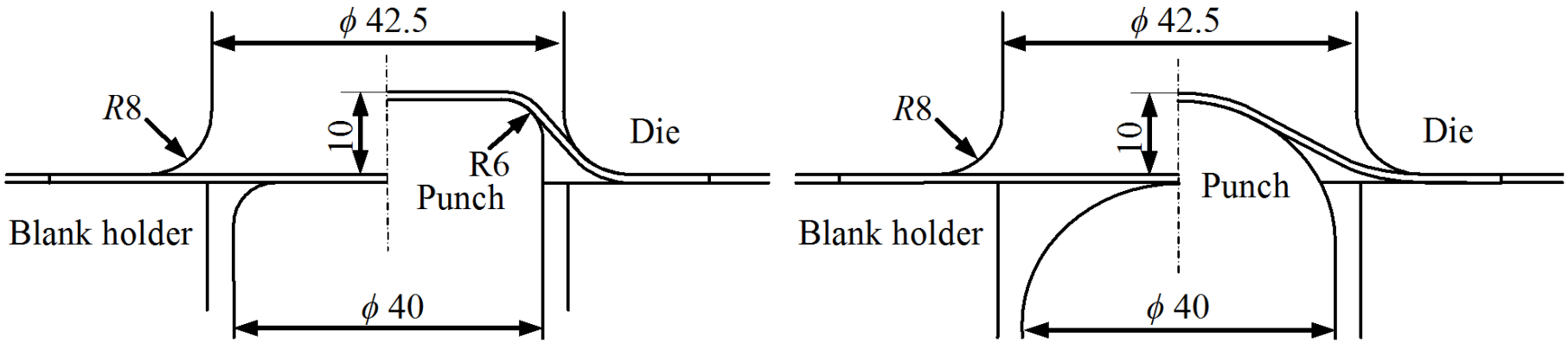

(a) Flat top shell specimen

(b) Hemispherical shell specimen

Fig. 2.2. Sheet drawing process.

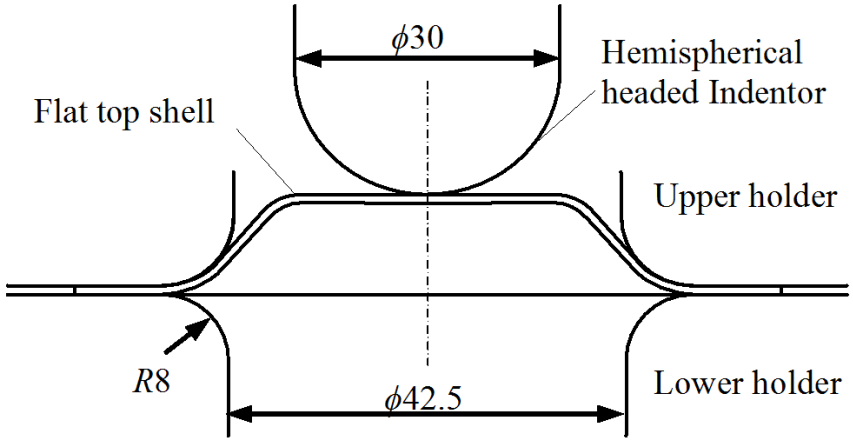

(a) FS: Flat top shell and hemispherical headed indentor

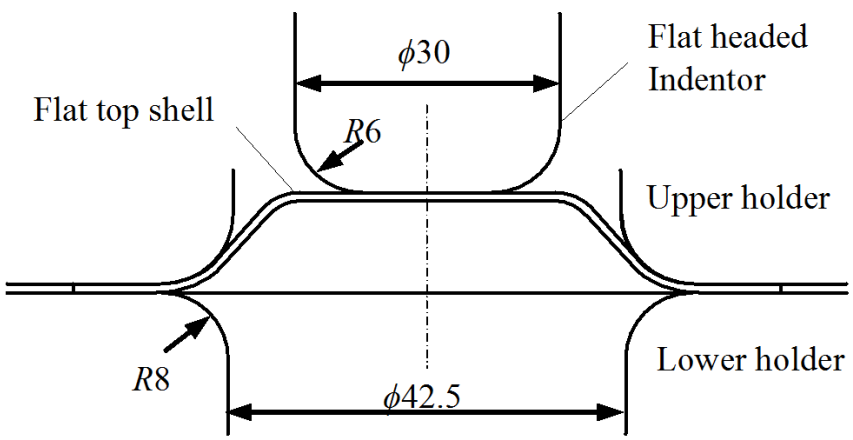

(b) FF: Flat top shell and flat headed indentor

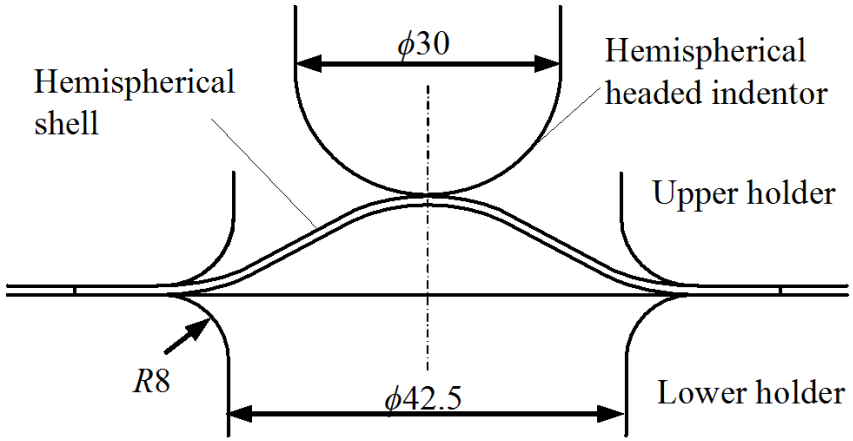

(c) SS: Hemispherical shell and hemispherical headed indentor

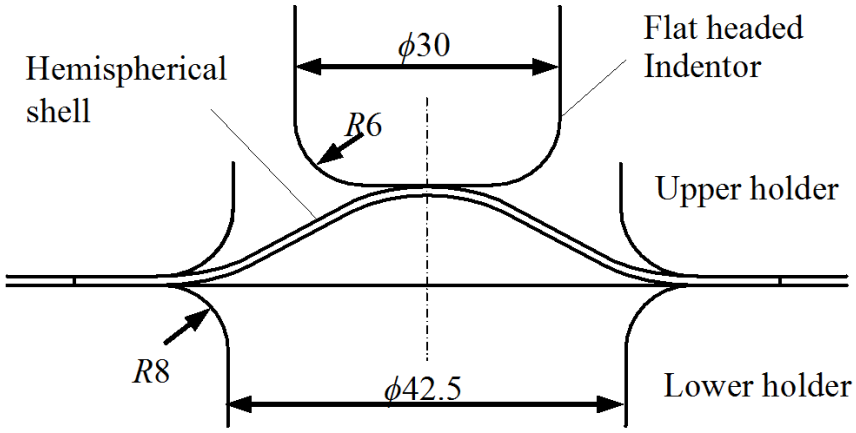

(d) SF: Hemispherical shell and flat headed indentor.

Fig. 2.3. Variation in combinations of formed shells and indentors.

2.3 Experimental results and discussions

Relationship between the collapse stroke and the force is most important characteristic in designing the press formed product as effective energy absorber. Fig. 2.4 demonstrates the progressive deformation patterns for 4 kinds of experimental conditions. The corresponding indentation force curves are shown in Fig. 2.5.

Deformation behavior of the flat top shell is first discussed. The hemispherical indentor gradually contacts the flat top part of the shell, thereby the concavity is formed on its top in FS condition. The indentation force gradually increases in the early deformation stage. The portion of the shell that was in contact with the die profile during press forming is unbent or flattened. On the other hand, the hat top corner portion contacted with the punch profile during forming decreases the radius. The indentation force once drops and takes minimum at around 22 mm indentation stroke, because the part outside the indentor becomes flat. Then the geometrical rigidity becomes low. The indentation force shows a rapid increase, when the shell wall deformation is extensional. Since the deformation behavior depending on the shell shape and the indentation condition is the exclusive concern in the study, the deformation in the extensional stage is excluded, though the energy is consumed in the deformation.

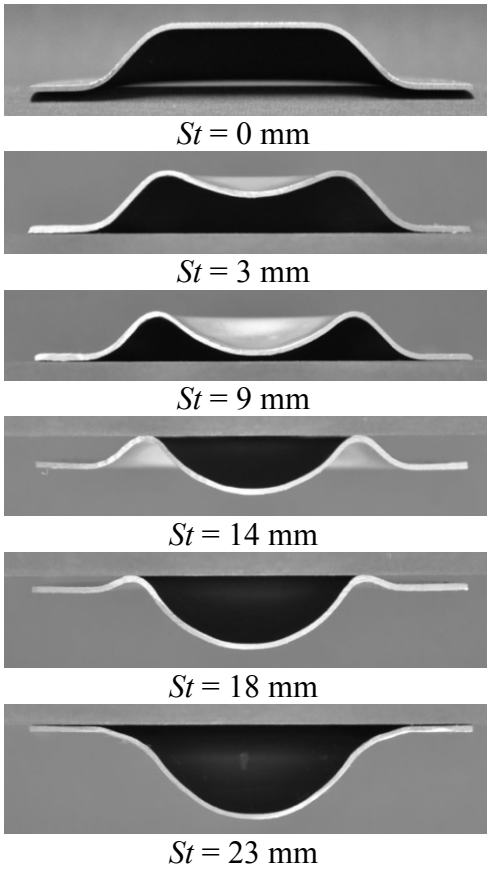

(a) FS

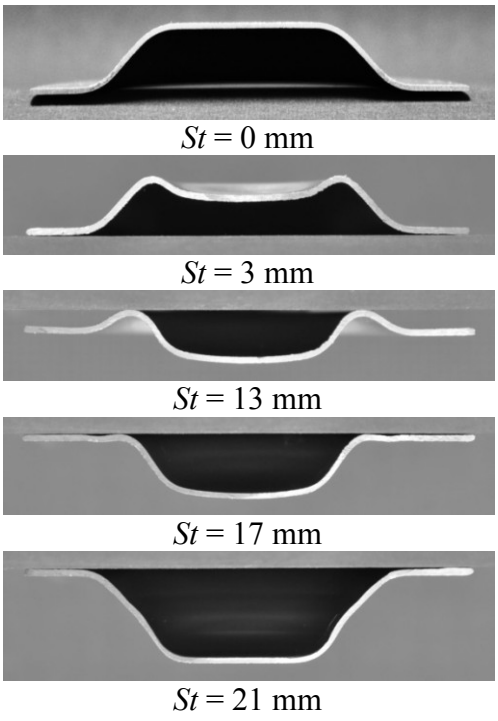

(b) FF

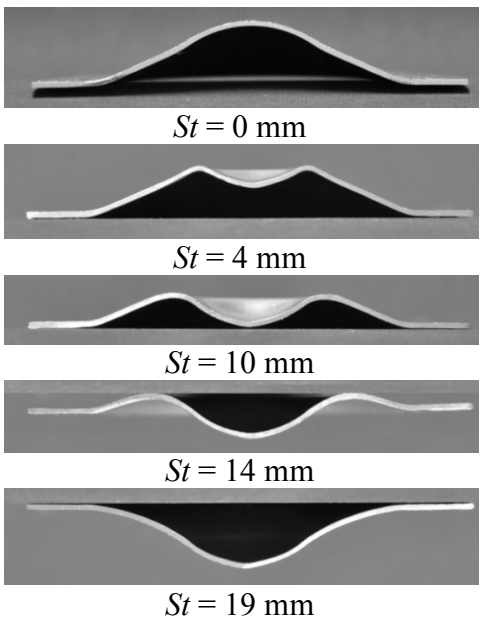

(c) SS

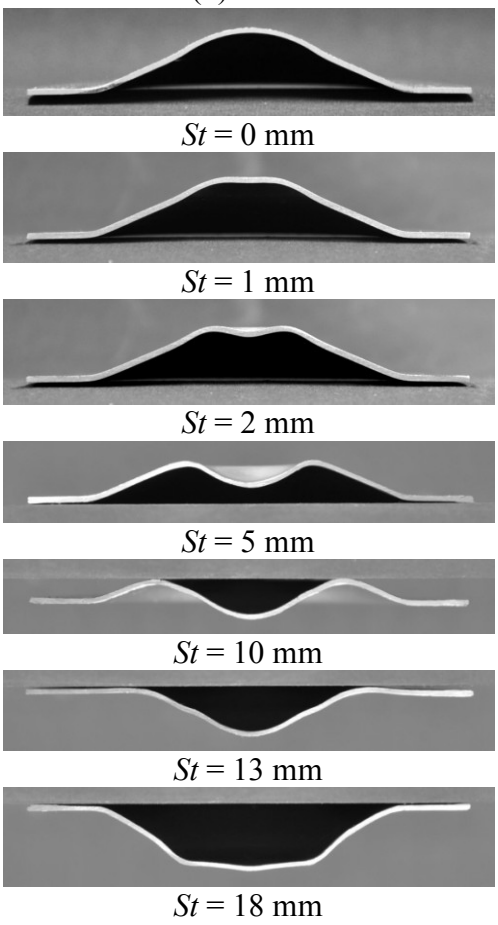

(d) SF

Fig. 2.4 Progressive deformation patterns under various indentation conditions (*St*: Indentation stroke).

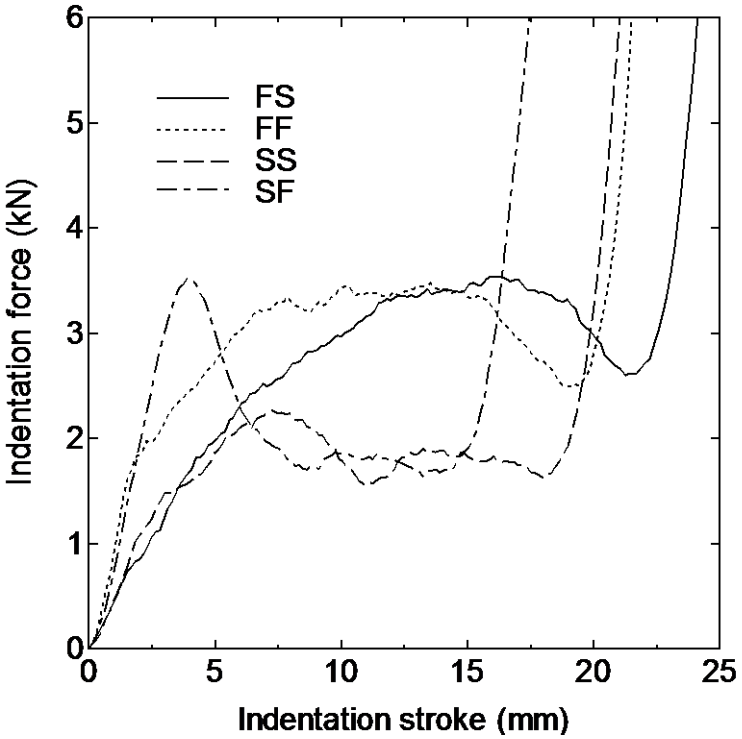

Fig. 2.5 Indentation force curves under various indentation conditions.

As for the FF condition, the force exhibits a steeper slope than that of FS in the early stage of indentation. The main deforming zone is the vicinity of the round corner of the indentor in the early stage, where the deformation is more extensive in comparison with that in FS. The maximum indentation force is almost comparable to that in FS. The indentation stroke at force drop is shorter in FF than that in FS. Drop and steep increase of the force also appear in FF for the same reason mentioned above.

Next, deformation of hemispherical shell specimen is discussed. In the case of SS condition, contact area increases with the increase of indentation force. The plastic hinge moves outward according to the contact position to the indentor. The force drop just before the sharp increase is not clearly seen. Variation in the force exhibits a plateau for the range from 10 to 18 mm stroke after a slight peak. This kind of force plateau is seen also in axial collapse of honeycombs and tubes, where the cyclic buckling lobes are formed. The stroke of the force plateau is not long, however, this kind of feature is often preferred for the shock absorbing component.

In the case of SF, the apex part of the hemispherical shell becomes flat increasing the contact area to the indentor as drawn by the solid line in Fig. 2.6. The in-plane compressive stress arises. Then the indentation force rapidly increases as shown in Fig. 2.5, because the deformation is constrained by the flat bottom of the indentor. When the stress reaches a certain critical level, the material begins to buckle. Such force increase is usually preferable in view of the improvement in the energy absorption performance per structural mass. When the stress reaches a certain critical level, the material begins to buckle then the bending deformation also contributes the deformation and the force level. The shell top flattens at about indentation stroke of 1 mm. The illustration of buckling is that in 2 mm stroke as observed in Fig. 2.4 (d).

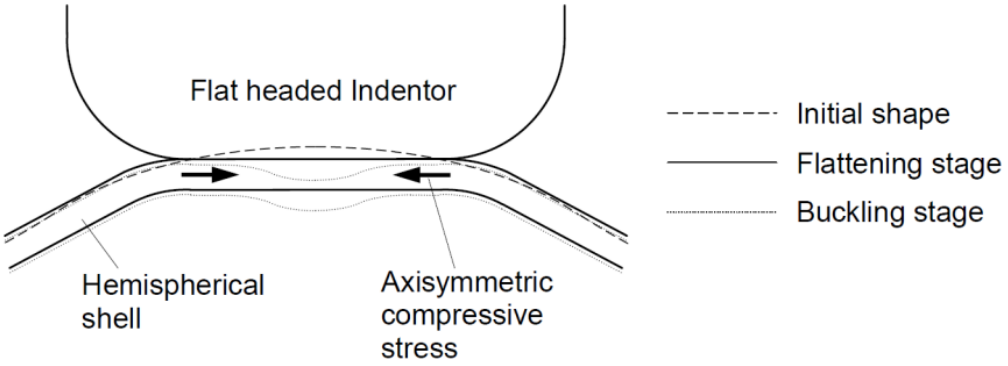

Fig. 2.6 Deformation behavior in early indentation stage of SF.

The force decreases showing a plateau after peak, whose level is comparable with that of SS, because both deformation modes are similar. The rounded portion formed by buckling finally becomes flat by the stretching of the periphery during the stage of sharp force increase. Comparing the general force variation for two shell shapes, it is greater in flat top shell than that in hemispherical one, because the structural rigidity is higher in flat top shell.

The consumed energy in indentation is recognized as an index of energy absorption performance. Generally speaking, deformation for energy absorption requires some space. The admissible space is usually considered to be the inner space of the shell. Hence, it may be appropriate to calculate the consumed energy in the travel length of the indentor equal to the shell height of 10 mm. The consumed energy E_C is defined in the form:

$$E_C = \int_0^{S_h} F(x)dx \tag{2.2}$$

where F is the indentation force and S_h is the shell height.

The consumed energy is presented in Fig. 2.7 for each deformation condition. It is largest in the case of FF. The increase ratio of the energy is about 30 % when the hemispherical indentor is replaced by a flat headed one in both shell shapes. Further, the performance of SF is comparable with the case of FS. This implies that the energy absorption performance is affected by not only product shape but also the crushing mode, which remarkably depends on the indentation manner.

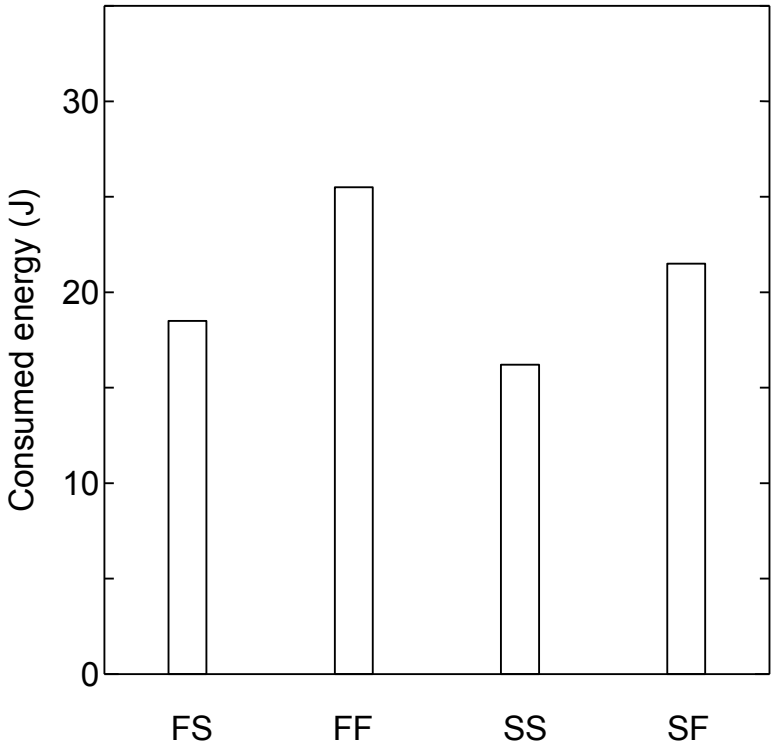

Fig. 2.7 Summary of consumed energy in indentation stroke equal to shell height.

2.4 Numerical simulation

2.4.1 Computational conditions

The numerical model is shown in Fig. 2.8, which corresponds to the experimental condition FS (combination of flat top shell and hemispherical indentor). The left figure is the general view of the 3D model describing elements of the tools and the sheet. The right one indicates their initial arrangements on symmetric plane. Dimensions of the numerical model are similar to those in experiment. The tools are described with shell elements whose mechanical property is assumed to be rigid. The elements of the sheet are described with the 14,336 hexahedron solid elements and the number of nodes is 18,245. The number of the layer through thickness is 4. This division number was used in the numerical simulations of other sheet forming processes by one of the authors, where the deformation behavior was appropriately predicted [28, 29]. In computation, the shell forming is first processed by the punch, while the indentor is stationary. After the shell forming, the punch moves backward 40 mm. Applied nodal forces on the shell surface contact with the punch decrease and eventually become 0 during the unloading process. Thus the shell is supported by the blank holder and the die. Subsequently, the indentor travels downward toward the shell.

The dynamic explicit finite element solver DYNA3D (public domain version) was used [30]. In order to apply the code to the quasi-static deformation, the speed-scaling technique is commonly introduced for this kind of solver. The technique is very effective for saving the computational time, where the tool speed is set to be much faster than the actual one. It is available unless the effect of material inertia arises. Therefore, the tool speed was determined before the calculation of indentation in the present study.

The isotropic elastic plastic material with *n*-th power strain hardening property was assumed for the sheet material. The friction of all interfaces was ignored. The punch speed was set to 5, 10 or 20 m/s for trial in speed scaling. The calculated punch force - stroke curves in the flat top shell forming are shown in Fig. 2.9 together with the experimental curves. The nodal forces of the punch in the moving direction are summed to obtain the punch force. General trend seems similar for these three speeds, all of which are generally agree with the experimental result. However, in the enlarged view of the early stage, the punch force indicates zero from 0.75 to 1.2 mm stroke in the case of 20 m/s punch speed, which means that the separation of the sheet from the punch occurs due to the excessive inertia of the material. Further, overshooting force at around 2 mm stroke is observed, which may also be explained by the same reason. On the other hand, the difference between 5 and 10 m/s conditions seems rather small. Therefore, the inertia effect under 10 m/s punch speed can be practically ignored, thus the tool speed was determined 10 m/s in view of the computational efficiency. The difference between the calculated shell height and the prescribed one due to spring back was as small as 0.05 mm. The effect is considered practically negligible.

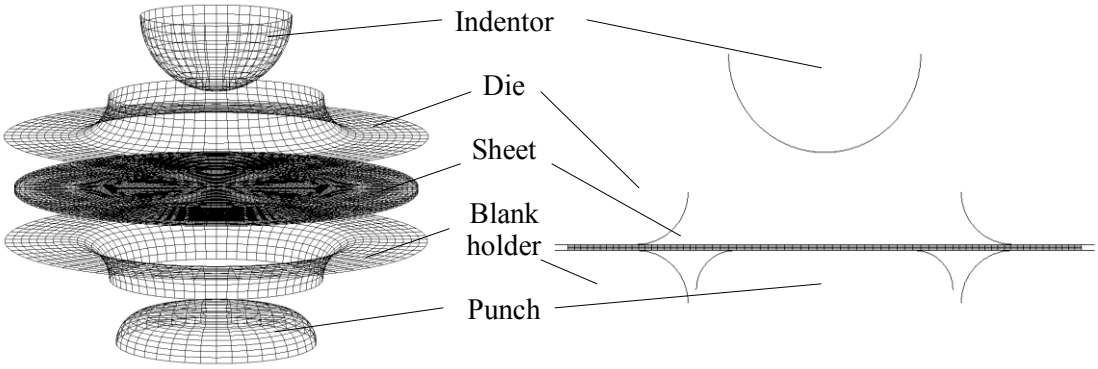

Model of parts Initial arrangement on symmetric plane

Fig. 2.8 Numerical model (FS: Flat top shell and hemispherical indentor).

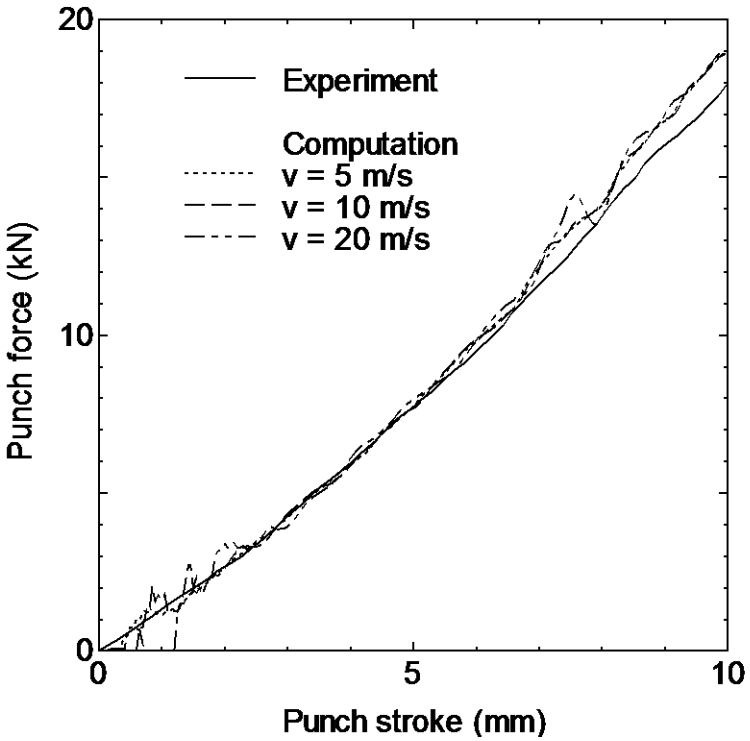

(a) Punch force - stroke curves

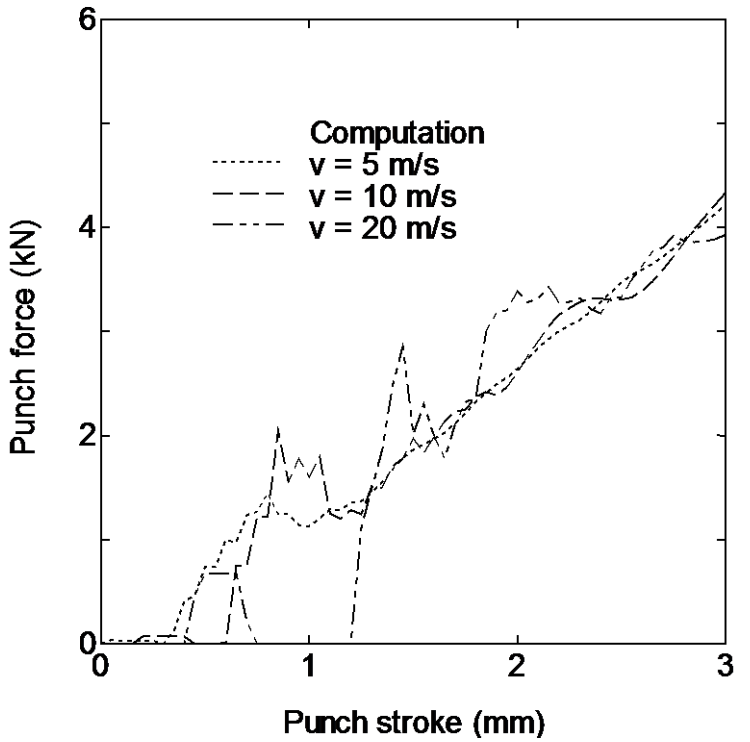

(b) Enlarged view of early forming stage

Fig. 2.9 Punch force – punch stroke curves in press-forming of flat top shell and calculated ones under 3 speed conditions (n = 0.15, C =383 MPa).

2.4.2 Computational results and discussions

The indentation force - stroke curves in computation and experiment are shown in Fig. 2.10 for FS condition. The force variation is qualitatively predicted with the rapid increase nearing the end of the stroke due to the stretch of the shell wall. However, the difference between these two conditions is obvious, where the calculated force is greater than that in experiment. This may be due to that the plastic hardening property of the material is assumed to be isotropic. Considering that the loading direction in the indentation process is opposite to that in the forming process and the rounded part bent by the die profile recovers to be flat, the Bauschinger effect of the material may arise. A series of tensile and compressive operations of soft A5052 aluminum alloy revealed that the Bauschinger effect in stress reversal appears as the plastic strain increases [31]. Consequently, the kinematic hardening plasticity may be more appropriate than the isotropic one. The kinematic linear hardening plasticity as shown in Fig. 2.11 is available in the solver code used here. The parameter β is set to 1 in isotropic hardening, and becomes less than 1 in kinematic hardening. Considering that the test material used here is the 1/4 hard or work-hardened one, the value 0 for the beta may be allowable.

The plastic property of the material has to be again determined considering the availability of linear hardening plasticity for the further calculation. For the purpose, it may be reasonable to compare the calculated press forming force with the experimental one conducting a parametric study changing the initial yield stress and the hardening modulus. The forming force in the linear hardening property of $\sigma = 210 + 420\varepsilon$ MPa well agrees with the results in the experiment and in the computation with isotropic n-th power hardening law as demonstrated in Fig. 2.12. These determined plastic parameters are used in the further computations.

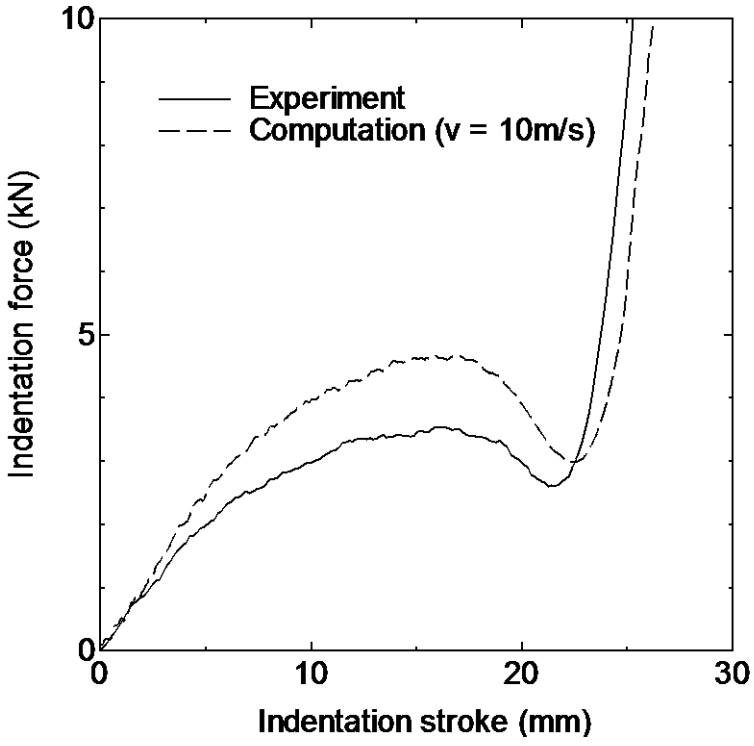

Fig. 2.10 Indentation force-stroke curves in FS.

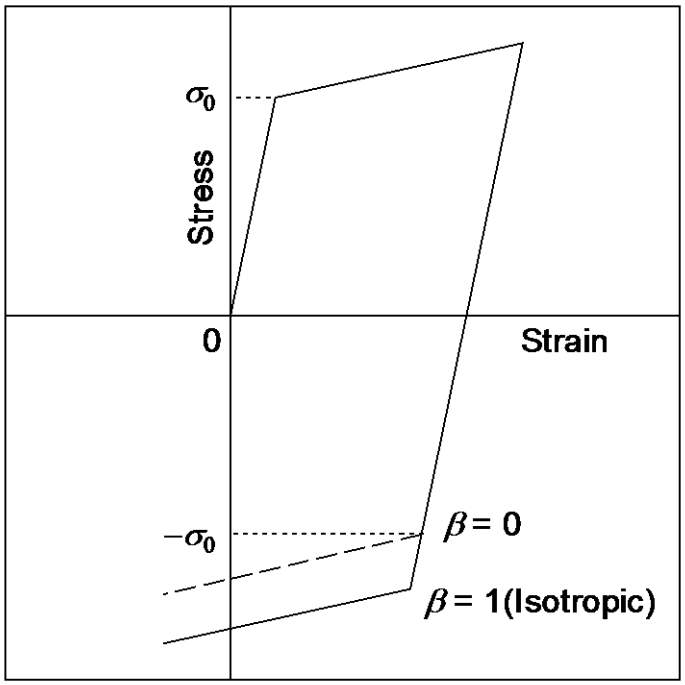

Fig. 2.11 Kinematic linear hardening plasticity.

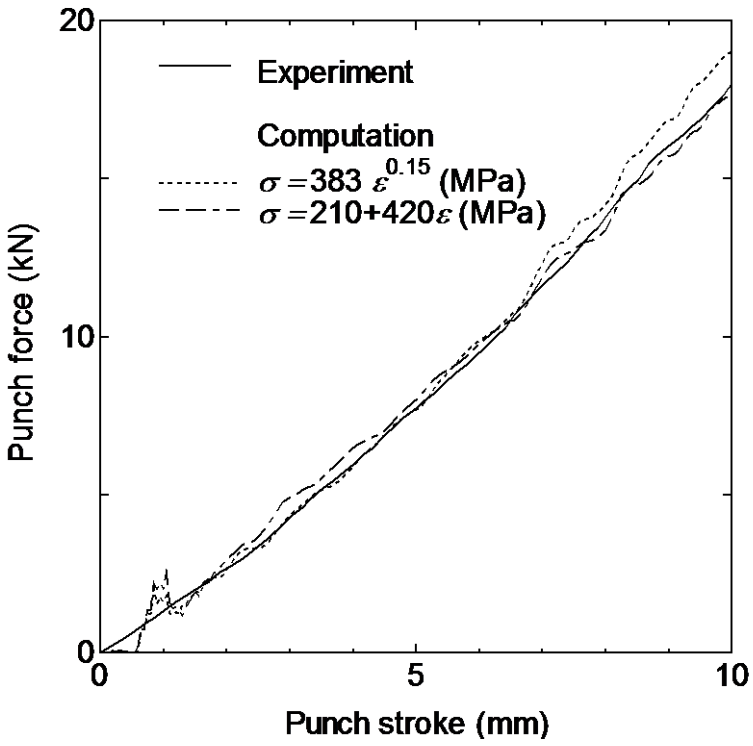

Fig. 2.12 Punch force – stroke curves in computation for two mechanical properties.

The force - stroke curves of indentation process for FS condition are drawn for β = 0, 0.5 or 1 in Fig. 2.13. The curve with β = 0 is generally close to the experimental result over the most indentation stroke, though the calculated force at concavity part is about 20 % smaller than that in experiment. In the further computation, the parameter β is set to 0.

Progressive deformation patterns are exhibited in Fig. 2.14 for each condition. The press forming process is the deformation stages 1 ~ 3, where the forming punch is also drawn. The indentation process is the stages 4 ~ 9, where the indentor is drawn. The deformation patterns predicted by computation are well consistent with the experimental result for all conditions. Fig. 2.15 shows the indentation force - stroke curves obtained by computation and experiment for each condition. Steeper force increase at the incipient stage is successfully simulated for FF and SF conditions (flat headed indentor), comparing with that for FS and SS conditions (hemispherical indentor). The force - stroke curve for the case of FS in Fig. 2.15 (a) is same to Fig. 2.13 except for the scale of vertical axis, in which the force is adequately predicted in the most indentation stroke as mentioned. The calculated force of FF is slightly greater than that of the corresponding experiment in Fig. 2.15 (b).

Further, the less variation in indentation force before the rapid force increase at the final phase is also successfully simulated in the case of SS as shown in Fig. 2.15 (c). It is noted that the initial peak force followed by the gradual decrease in the case of SF is also properly predicted as shown in Fig. 2.15 (d). This phenomenon is because of the buckling of the material in front of the indentor head as demonstrated in the stages 4 and 5 of SF in Fig. 2.14.

The consumed energy by the deformation is shown in Fig. 2.16, whose value corresponds to the area under the indentation force – stroke curve. The predicted values are almost comparable with those in experiment. However, considering that the friction is ignored in calculation and the linear hardening model is used, there is a room for improvement.

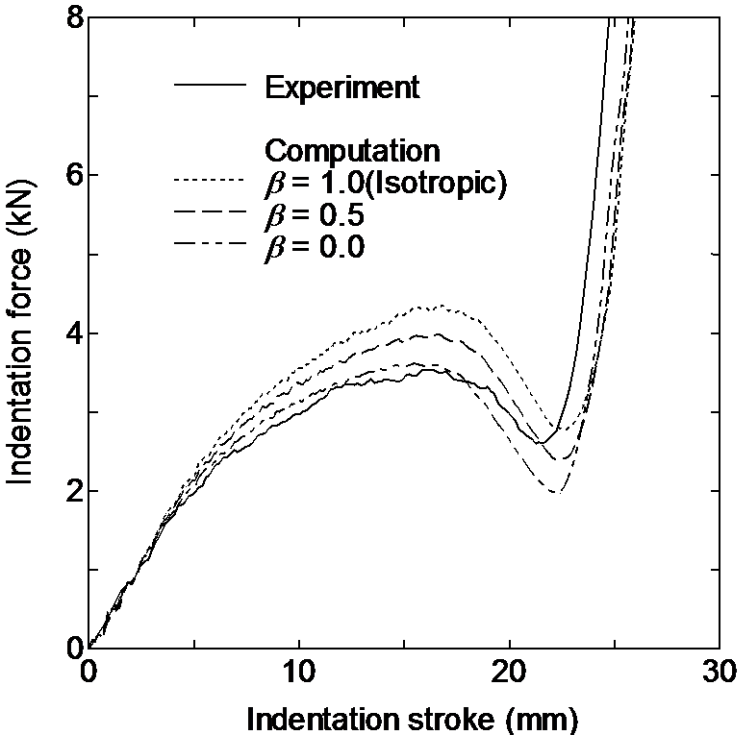

Fig. 2.13 Indentation force – strokes curves for isotropic or kinematic hardening property.

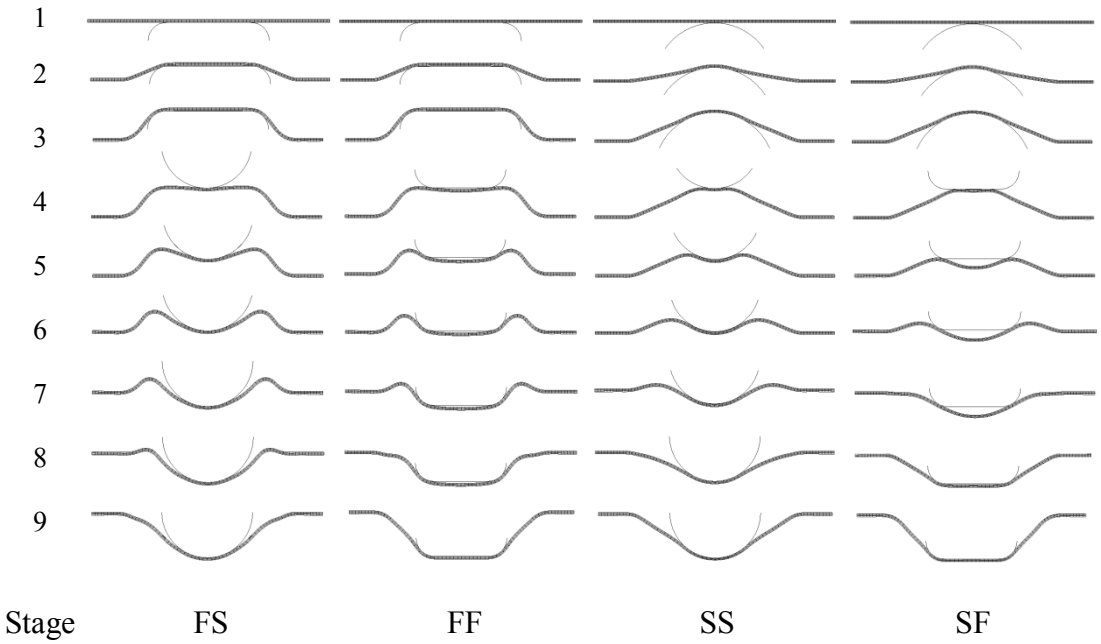

Fig. 2.14 Progressive deformation patterns in computation, Stage 1 ~ 3: Forming process, Stage 4 ~ 9: Indentation process, Indentation stroke: 1, 5, 10, 15, 20, 25 mm (Stage 4 ~ 9).

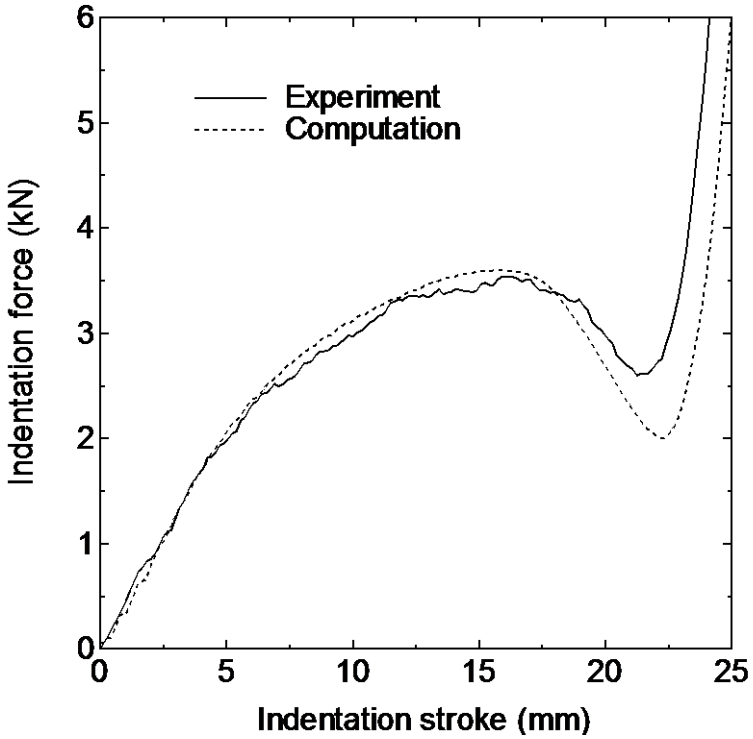

(a) FS

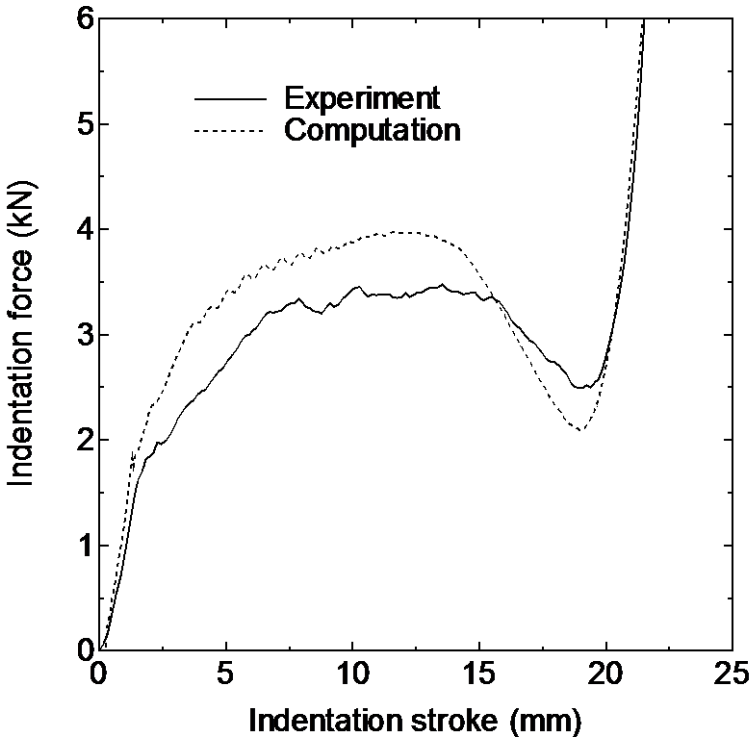

(b) FF

Fig. 2.15 Indentation force – stroke curves obtained in experiment and computation for various indentation conditions.

(to be continued)

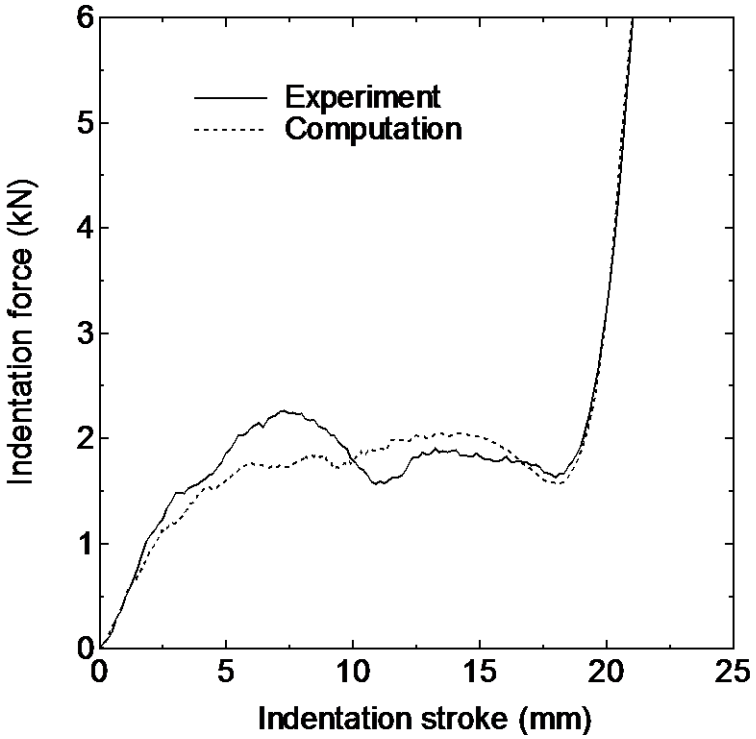

(c) SS

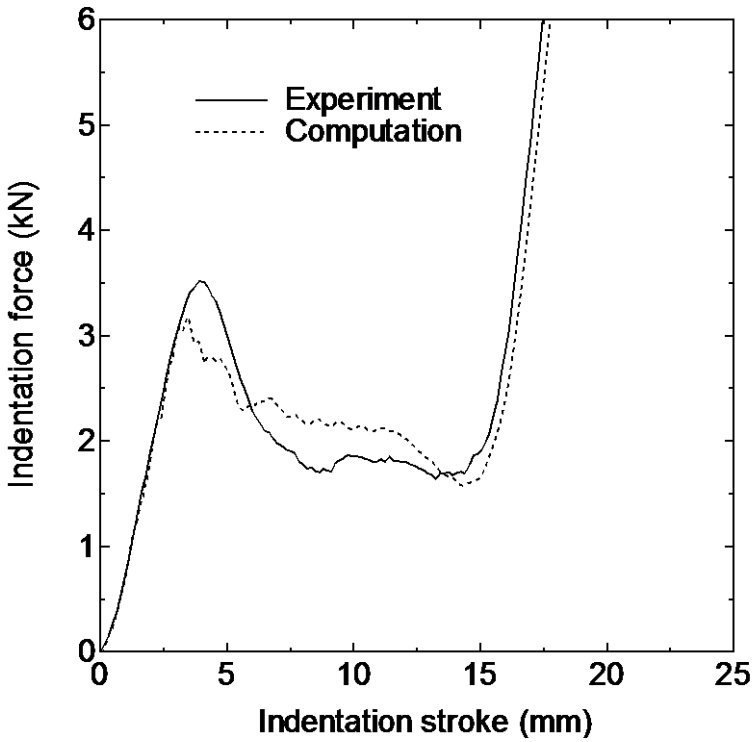

(d) SF

Fig. 2.15 (continued)

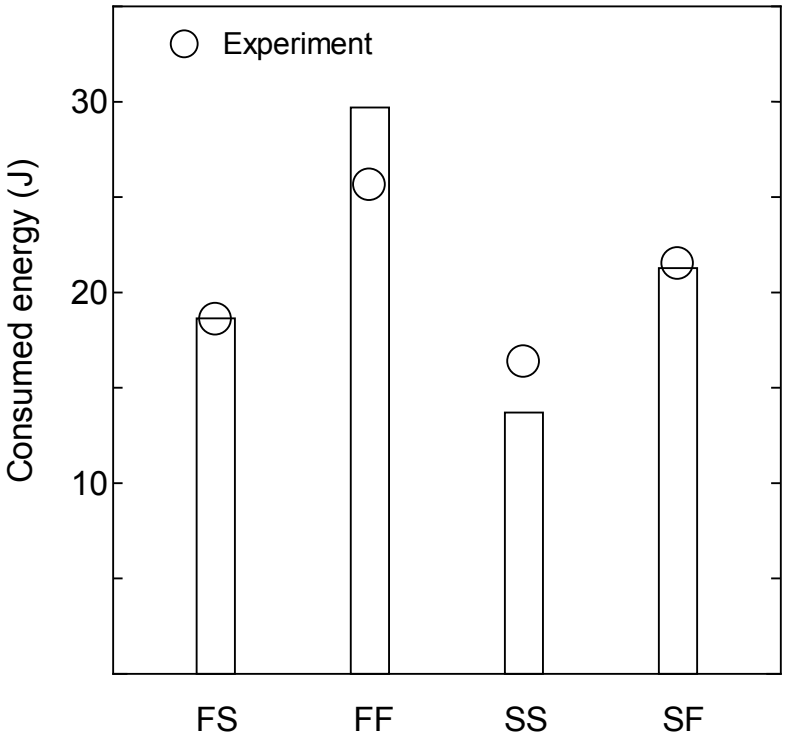

Fig. 2.16 Calculated consumed energy in indentation stroke equal to shell height.

2.5 Conclusions

Flat top and hemispherical aluminum alloy A5052 shells fabricated by the press forming were deformed by the flat or hemispherical headed indentor. Deformation patterns and characteristic of the indentation force were investigated. Energy absorption performance in indentation deformation of the shells was estimated for indentation stroke corresponding to the shell height. Numerical simulation was also carried out.

The energy absorbing performance of the shell was greater in the case of flat headed indentor than in the case of hemispherical one. Axisymmetric plastic buckling deformation under in-plane axisymmetric compressive stress field was found very effective for the increase of the resistance to collapse. When the hemispherical shell was deformed by similar shaped indentor, less force variation was achieved due to the appropriately generated mobile plastic hinge. The deformation patterns obtained in experiment were well simulated by the finite element calculation. The accuracy in prediction of indentation force was improved by introducing the kinematic hardening plasticity in the material constitutive model, on the other hand, the force was overestimated when isotropic plasticity was applied. Bauschinger effect is one of the considerations in designing the press formed parts used as energy absorbing component.

In the present study, several basic characteristics in the indentation behavior were revealed for the simple collapse conditions, they may provide some helpful guidelines in designing the collapsible parts and structures.

Chapter 3: Energy Absorption Performance of Press-Formed Shell under Impact (Elsevier, Procedia Engineering, Vol. 81(2014), pp. 951-956) [35]

3.1 Introduction

The present study is focused on the energy absorbing performance of press formed shell. The objective is to obtain the basic information for construction of the guidepost in designing the energy absorber. The shape of the press formed shell is flat top or hemispherical. The materials were mild steel SPCE and aluminum alloy A5052-H34 sheets. Indentation was conducted using the flat or hemispherical headed indentor under impact condition using a drop hammer or quasi-static one.

3.2 Test material and experimental procedure

The test materials are aluminum alloy sheet A5052-H34 with 1 mm thickness and mild steel sheet SPCE with 0.8, 1.2 or 1.6 mm thickness. Their mechanical properties are listed in Table 3.1. Square sheets of 90 x 90 mm^2 was cut out from the original material sheet, and into circular sheet blank with 80 mm diameter using lathe or wire cut electro discharge machine. Finally, it was press-formed into desired shaped using hydraulic deep drawing testing apparatus, shown in Fig. 2.1, as illustrated in Fig. 3.1. The formed height is 10 mm for both aluminum alloy and mild steel SPCE. The shape of specimen is flat top or hemispherical shell. The shape of indentor is flat headed or hemispherical Flat head or hemispherical headed indentor was used to fabricate the shell. The combinations of shells and the indentors are shown in Fig. 3.2. The abbreviated notations FS, FF, SS and SF are used. The first letter represents the shell shape, F: 'F'lat top or S: hemi'S'pherical shell. The latter represents the indentor, F: 'F'lat headed or S: hemi'S'pherical headed indentor. It should be noted that, dice hole diameter was 42.5 mm, dice holes radius corner was 8 mm. For flat headed indentor, diameter 40 mm, with radius corner 6 mm, and for hemispherical headed indentor, diameter 40 mm was used to fabricate the shells. To determined the most appropriate blank holding forces for fabricating, Siebel's formula noted in chapter 2 explained in eq. (2.1) was used to calculate the surface contact pressure. It gives the minimum blank holding force without flange wrinkling. Each material's blank holding force are shown in Table 3.2. Lubricant oil by Nihon Kohsakuyu Co.,LTD were applied to all tool and material interfaces when press-forming the shells.

Table 3.1. Mechanical properties of test materials.

Material (Thickness)	Ultimate tensile strength (MPa)	*c* (MPa)	*n*-value	Total elongation (%)
A5052-H34(1.0mm)	248.2	399.1	0.148	8.0
SPCE(0.8mm)	310.1	565.3	0.252	48.0
SPCE(1.2mm)	309.4	551.0	0.238	48.3
SPCE(1.6mm)	284.4	502.7	0.233	51.5

Work hardening property of *n*-th power law: $\sigma = c\varepsilon^n$

Table 3.2. Blank holding force and experimental parameters.

	D (mm)	d (mm)	t	β	δ	A (mm)	B.H.F (Nf)
A5052	80	40	1.0	2	40.0	2338.7	3482.8
SPCE	80	40	0.8	2	50.0	2338.7	4533.4
SPCE	80	40	1.2	2	33.3	2338.7	4220.3
SPCE	80	40	1.6	2	25.0	2338.7	3741.4

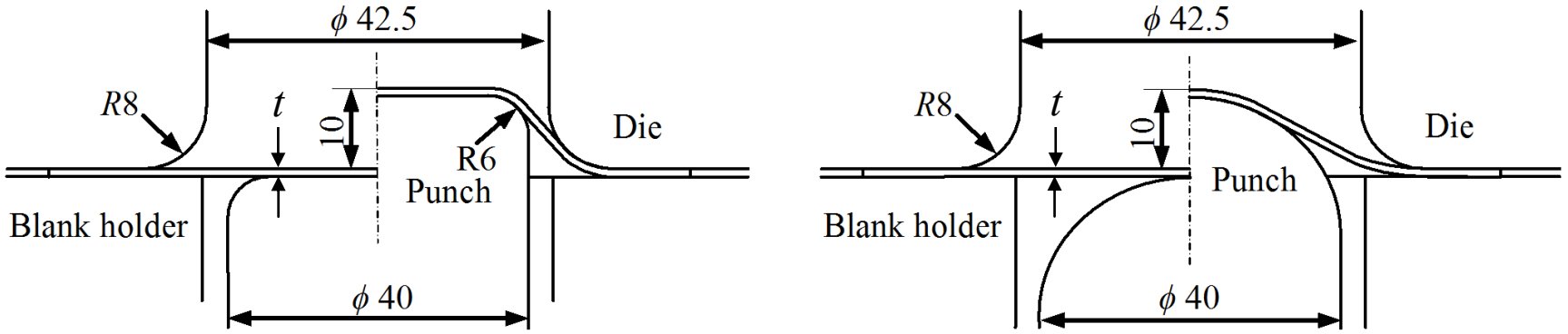

(a) Flat top shell specimen

(b) Hemispherical shell specimen

Fig. 3.1. Sheet drawing process of aluminum alloy (Initial thickness, t = 1.0 mm) and mild steel (t = 0.8, 1.2, 1.6 mm).

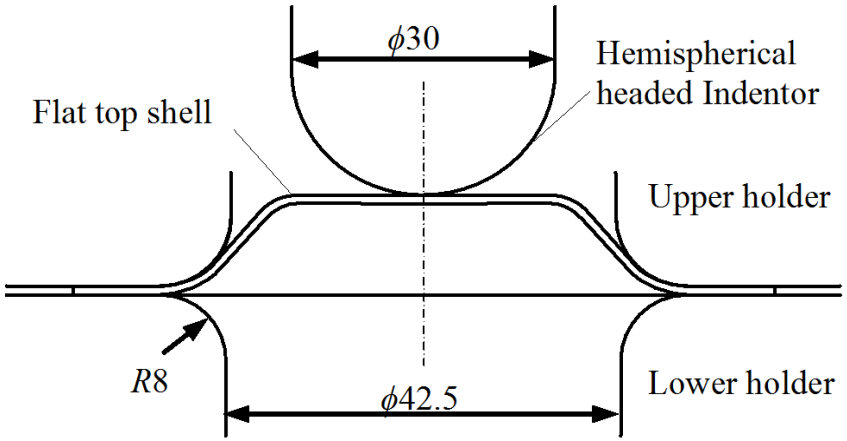

(a) FS: Flat top shell and hemispherical headed indentor

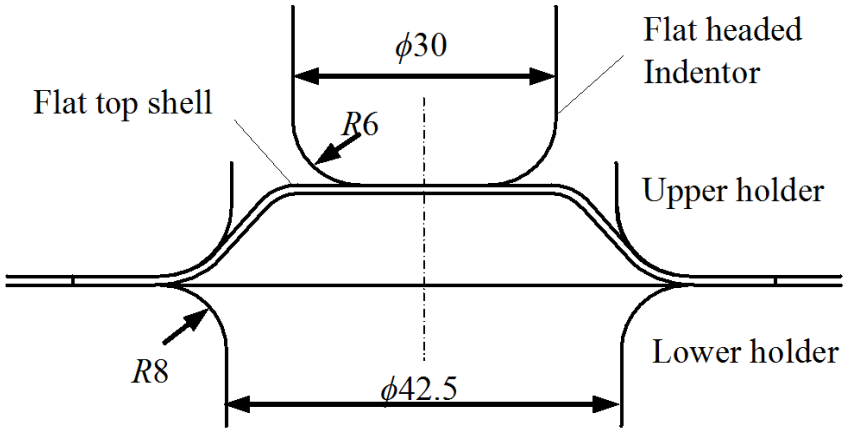

(b) FF: Flat top shell and flat headed indentor

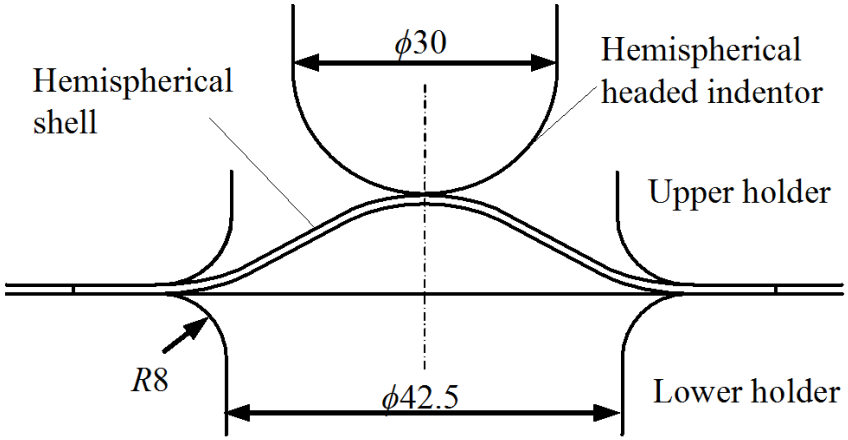

(c) SS: Hemispherical shell and hemispherical headed indentor

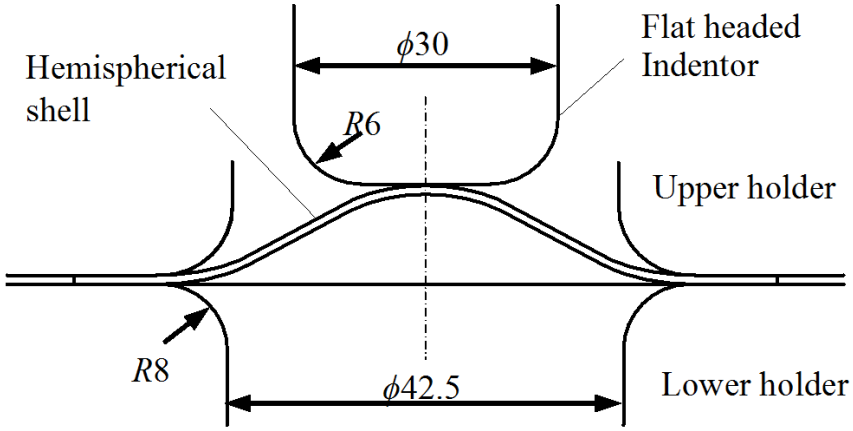

(d) SF: Hemispherical shell and flat headed indentor

Fig. 3.2. Variation in combinations of shells and indentors. (Indentor diameter, I_d = 30 mm)

Drop-hammer type impact testing machine (3.5 kN·m, Tokyo Testing Machine Incorporated) was used in impact compressed test. Impact indentation test was performed using 15 kg drop hammer with the indentor. General view of the impact testing apparatus is shown in Fig. 3.3 (a). Illustration of the testing part is shown in Fig. 3.3 (b) in which shell specimen is mounted.

Drop-hammer is impacted to the shell top with the impact velocity of 3.4 m/s (for aluminum alloy, A5052-H34) and 5.0 m/s (for mild steel, SPCE).

The indentation force generated from the compressed impact was collected by high speed high sensitivity load cell (handmade load cell using semi-conductor strain gage by KYOWA KSN-6-340-E4). Using this semi-conductor strain gage, the sensitivity is increase about 50 times than that of the conventional one.

Falling position of the drop hammer was measured by the laser displacement device (SUNX, HL-C1-WL). Impact load data amplified with high frequency signal conditioner (KYOWA Electronic Instruments Co., Ltd., CDA700) and laser measurement data were storaged directly in the computer memory using digital osciloscope (KENWOOD, PCS-3200)

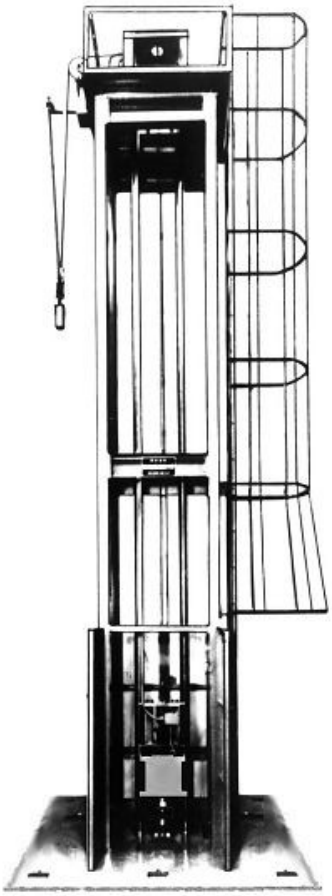

(a) General view

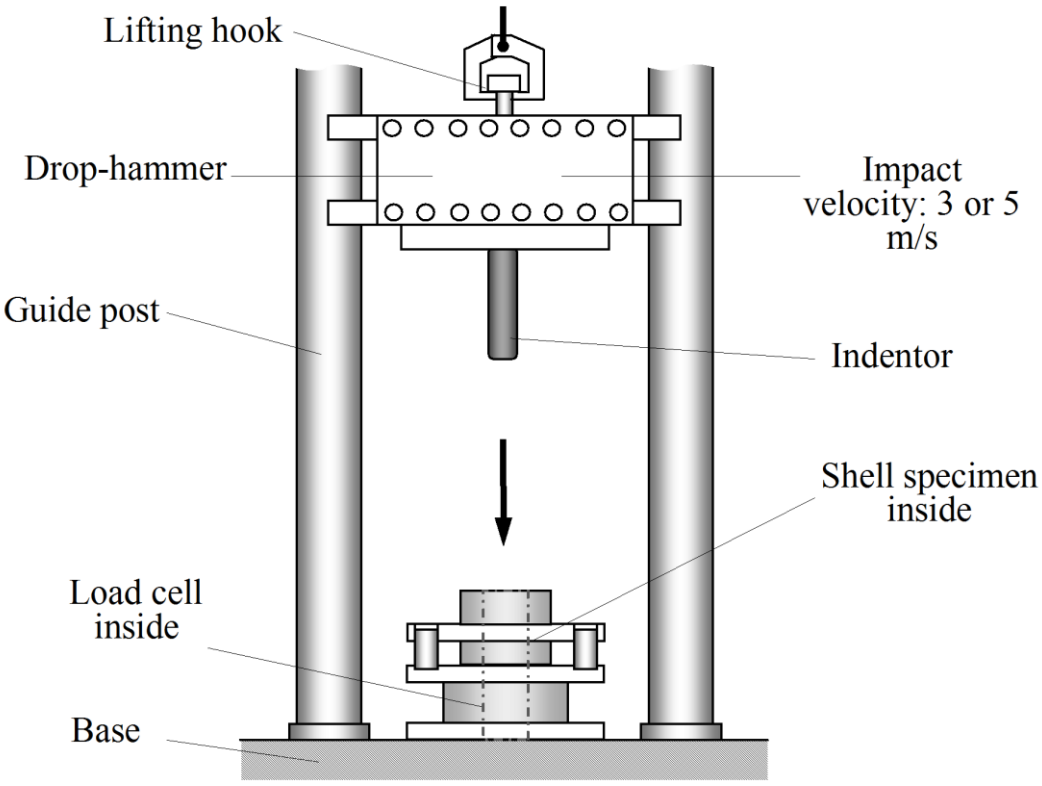

(b) Testing part.

Fig. 3.3. Drop-hammer type impact testing apparatus and testing part.

3.3 Experimental results and discussions.

Deformation behavior of flat top shell is first discussed. The SPCE shell hardened at most about 20 % in Vickers hardness scale, whose *n*-value is larger than that of A5052-H34. The example of the progressive deformation patterns of SPCE shell and the force curves under impact or quasi-static condition are summarised in Fig. 3.4. The deformation patterns are those obtained in quasi-static test, because the impact test can not be terminated at the desired indentation stroke. Variation in the indentor force during collapse deformation is an important property of the energy absorber. The force rapidly increases in the latter stage, where the shell shape is invertedand the shell wall undergoes tension. Such extensional deformation stage is not considered in the study. The impact force curve terminates before the rapid increase in the case of 1.6 mm sheet thickness. Because the motion energy of drop hammer is exhausted before it.

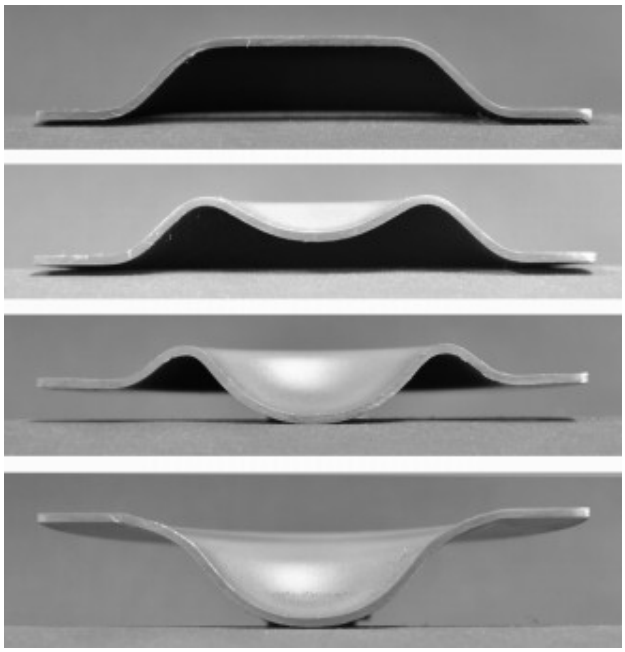

Deformation patterns
(a) FS deformation condition

Fig.3.4. Progressive deformation patterns of flat top shell and force curves in indentation.

(to be continue)

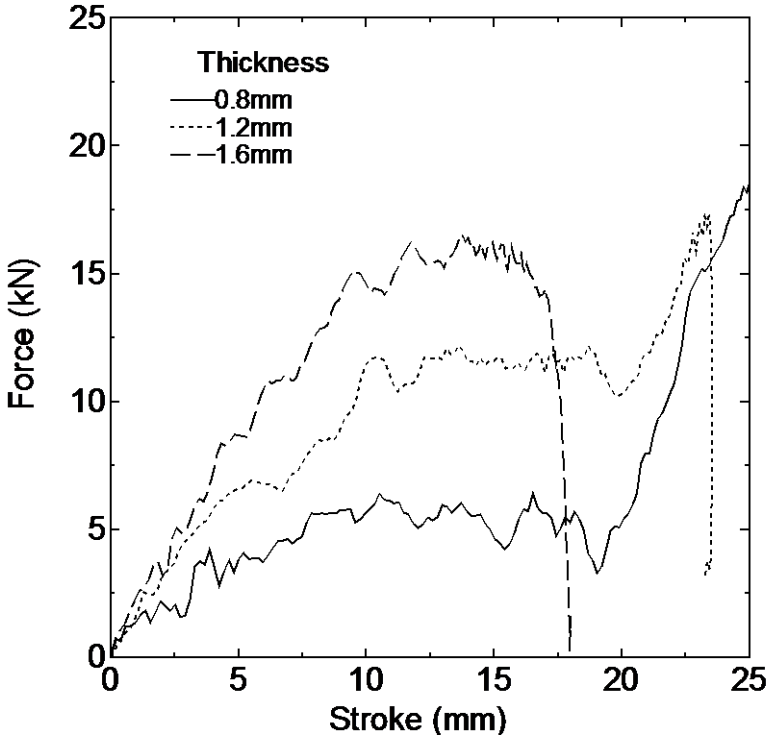

Impact test

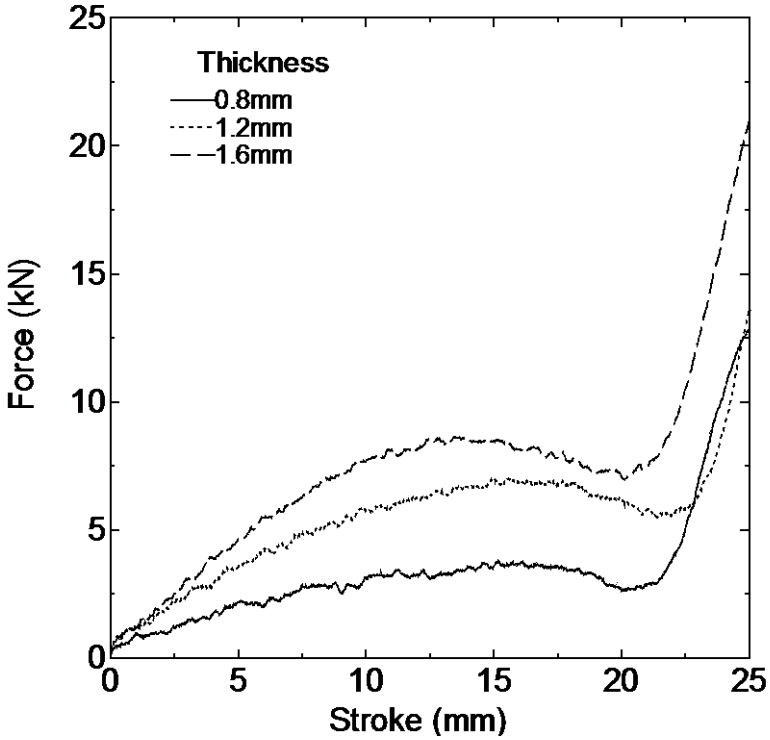

Quasi-static test

(a) FS deformation condition

Fig.3.4. (continued)

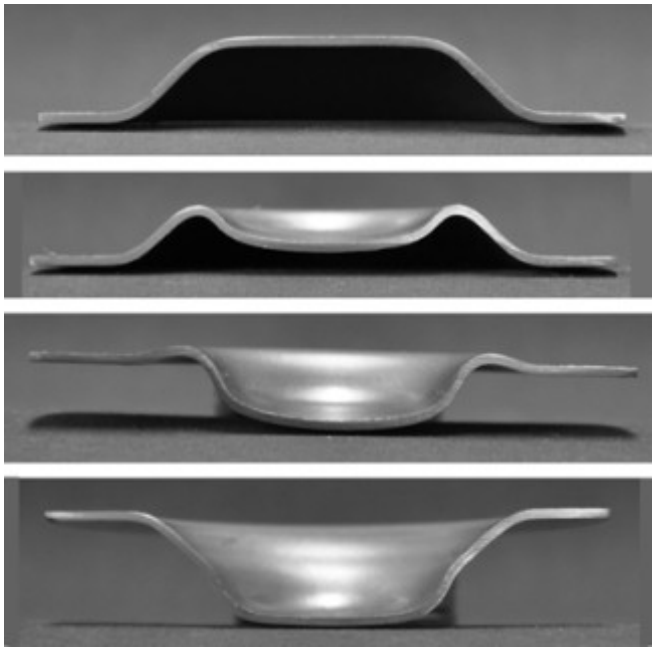

(b) FF deformation condition

Fig.3.4. (continued)

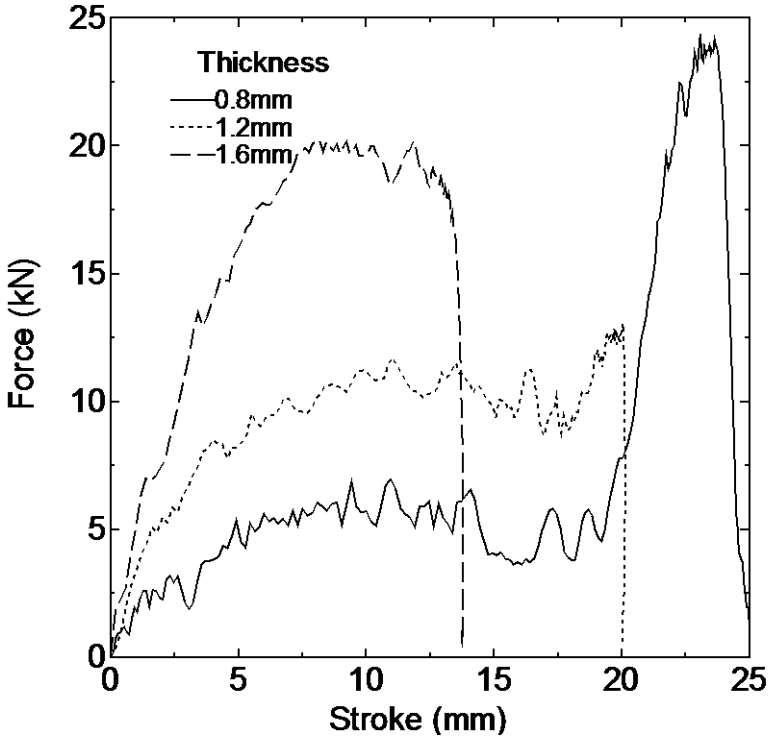

Impact test

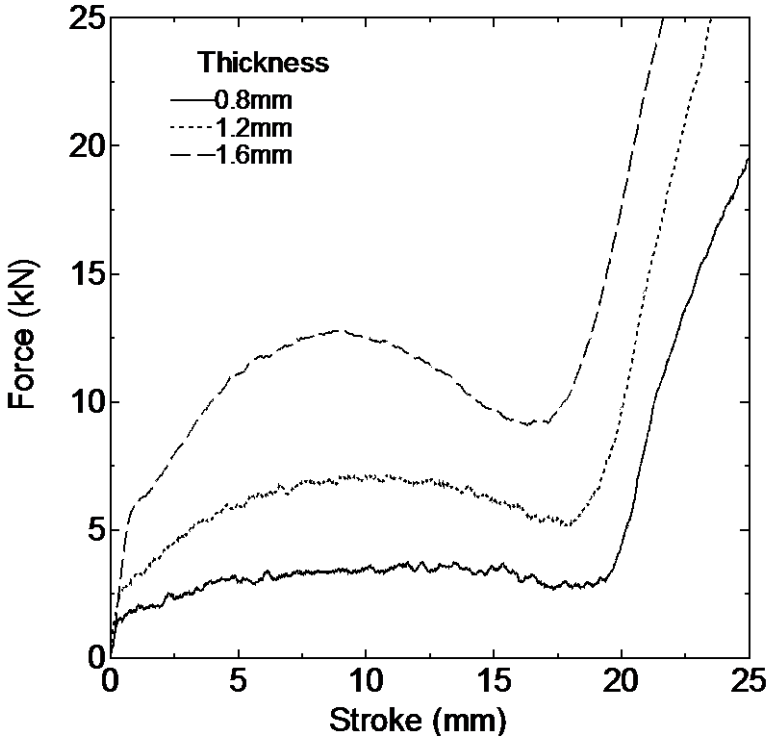

Quasi-static test

(b) FF deformation condition.

Fig.3.4. (continued)

The hemispherical indentor gradually increases the contact area at the flat top part of the shell. Then the indentation force also more gradually increases in the concavity formation stage under FS deformation condition than that under FF. The transition from elastic to plastic regime is sharp under FF condition, where the contact area of the shell to the indentor is almost unchanged in the early stage of the deformation. The bent portion of the shell in contact with the die profile portion becomes flattened, where the force drop is observed. The significant effect of sheet thickness in indentation force is observed.

The force in impact test is generally 1.5 times higher than that in quasi-static test. The strain-rate in indentation is roughly estimated to be around 100 /s. According to A. Niknejad [6] and Corbett [18], dynamics load show a higher values than those in quasi-static loads due to inertia effects, however the mild steel originally does not exhibit such high strain-rate sensitivity in the strain-rate of this order. The phenomenon observed in the present study implies that not only the indentation force on shell was increased due to cold work strengthening obtained in press-formed process [2] but also the strain-rate effect of mild steel, SPCE on the yield stress is enhanced if the loading direction alters.

The deformation behaviour of hemispherical shell is discussed below. The deformation patterns and the indentation force curves are exhibited in Fig. 3.5. Deformation patterns exhibited in the figure were in good agreement with the deformations and stress for elastic shells and its bifurcation point studied by Updike, Kalnins [32, 33] where hemispherical shells buckled when compressed against rigid plates. The forces are smaller than those of the flat top shell for the similar indentor. Less fluctuation in indentation force is observed for 0.8 and 1.2 mm sheet thickness under quasi-static SS deformation condition. The constant force is commonly preferable for the property of shock absorber. The reason of the less force fluctuation may be understood by observing how the mobile plastic hinge behaves. Shariati [24] concluded that increased shell thickness may affect plastic hinge radius. The result obtained in the present study also shows the same tendency, where the larger hinge radius becomes in the deformation patterns, thus the bending force becomes lower as the indentor strokes. On the other, the hinge length increases. In the deformation, the increase of hinge length and the decreasing bending resistance compensate each other in terms of indentation force. Therefore, the force is consequently maintained almost constant. The force under impact is greater than that in quasi-static deformation. However, the force plateau is seen only for the case with 1.2 mm sheet thickness. The tendency in force variation for the case with 1.6 mm thickness does not agree with that of quasi-static test. This may be attributed to the difference in deformed shape under the enhanced strain-rate effect mentioned above, though the shapes under impact could not be observed.

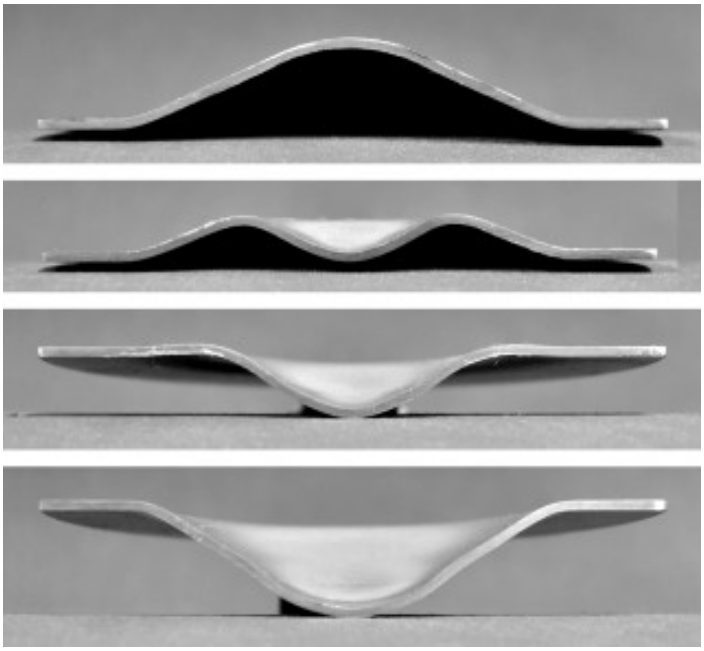

Deformation patterns

(a) SS deformation conditions

Fig.3.5. Progressive deformation patterns of hemispherical top shell and force curves.

(to be continue)

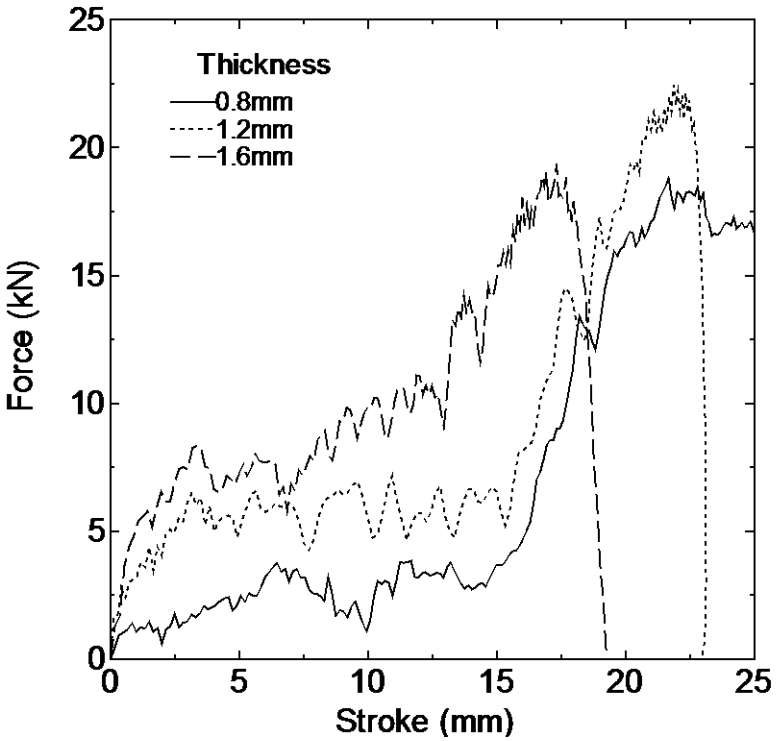

Impact test

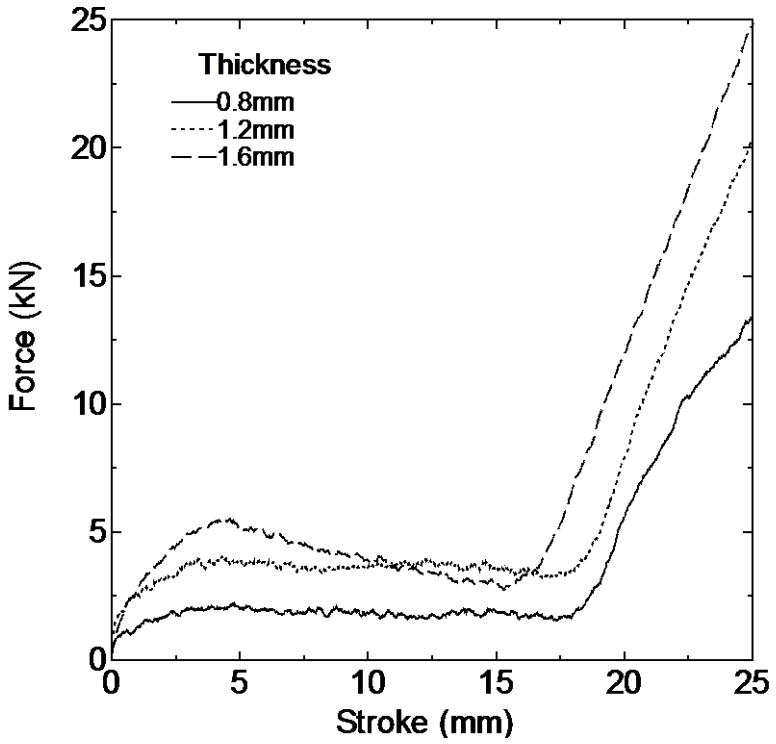

Quasi-static test

(a) SS deformation conditions

Fig. 3.5. (continued)

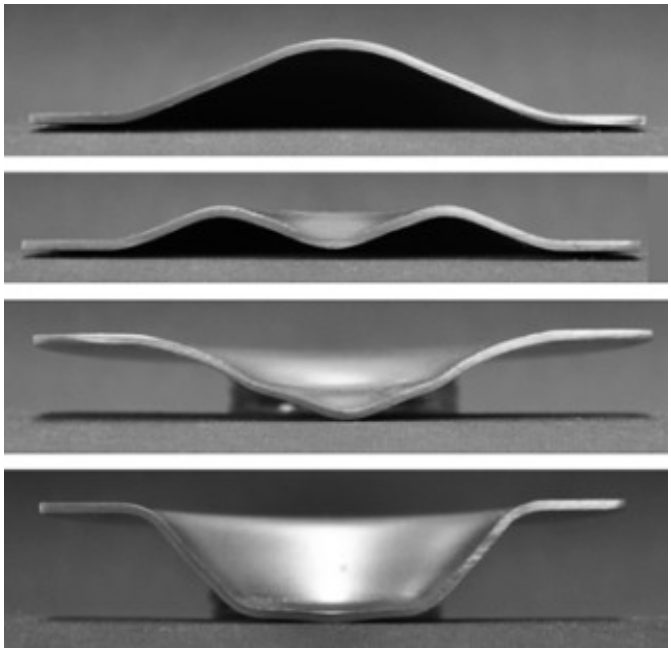

Deformation patterns

(b) SF deformation conditions

Fig. 3.5. (continued)

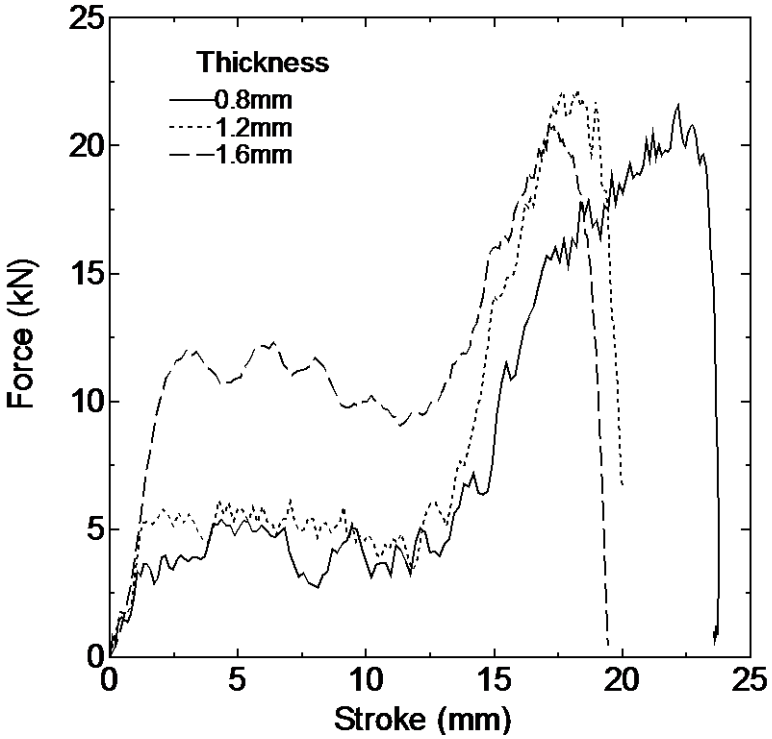

Impact test

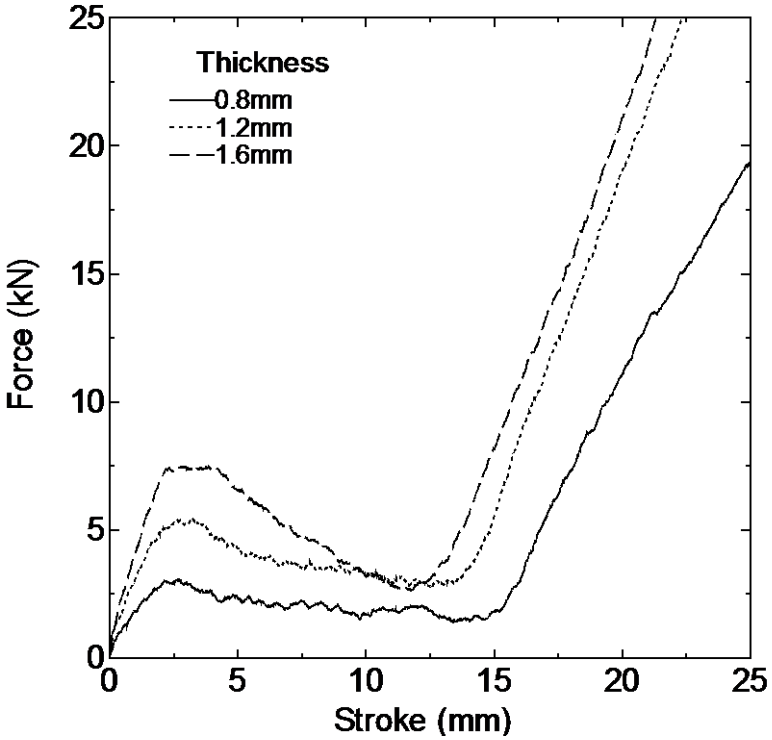

Quasi-static test

(b) SF deformation condition.

Fig. 3.5. (continued)

Figure 3.6 shows the force curves for aluminium alloy A5052-H34. The force levels are comparable for both strain-rate conditions. The most effective deformation condition is also FF deformation condition. The initial peak force appears under SF deformation condition. The reason is explained as follows: The round top portion is flattened by the flat headed indentor in the early stage of deformation. The axisymmetric compressive stress accordingly arises. The flattened part buckles beyond a certain stress. Therefore, the indentation force increases. It is found that the introduction of in-plane compressive stress is very effective in improving the energy absorption performance. The SS deformation condition provides the relatively stable indentation force as observed in SPCE.

Indentation force variation depends on the mechanical property of the material and the current shape or the structural rigidity. The force drop is caused by losing the structural rigidity as the shape flattens. It is generally observed that the drop is more supressed in SPCE(t=1.2) than that in A5052-H34(t=1) in Figs. 3.4, 3.5 and 3.6. The SPCE material exhibits larger strain hardening than A5052-H34 as shown in Table 3.1. In consequence, the force drop is compensated to a certain degree by the hardening property.

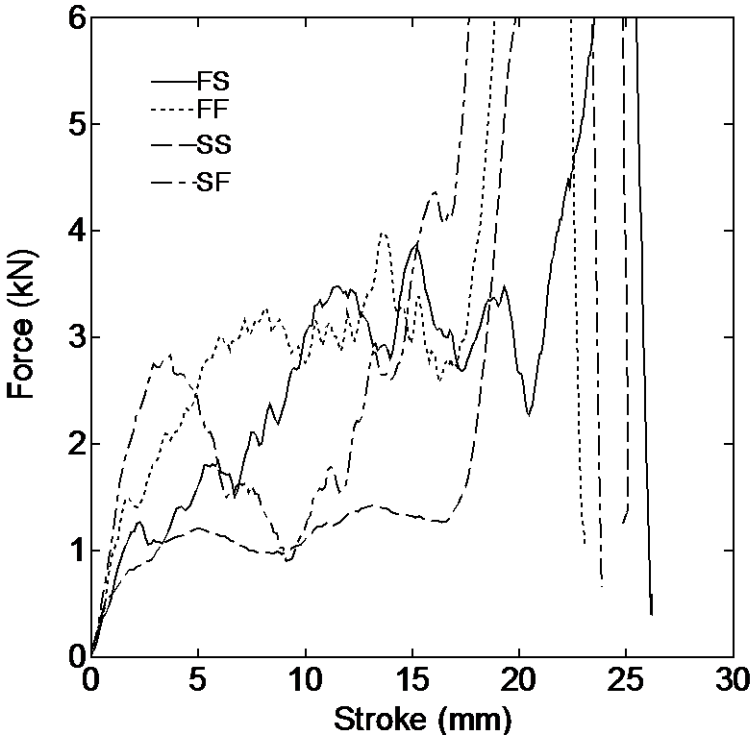

(a) Impact test

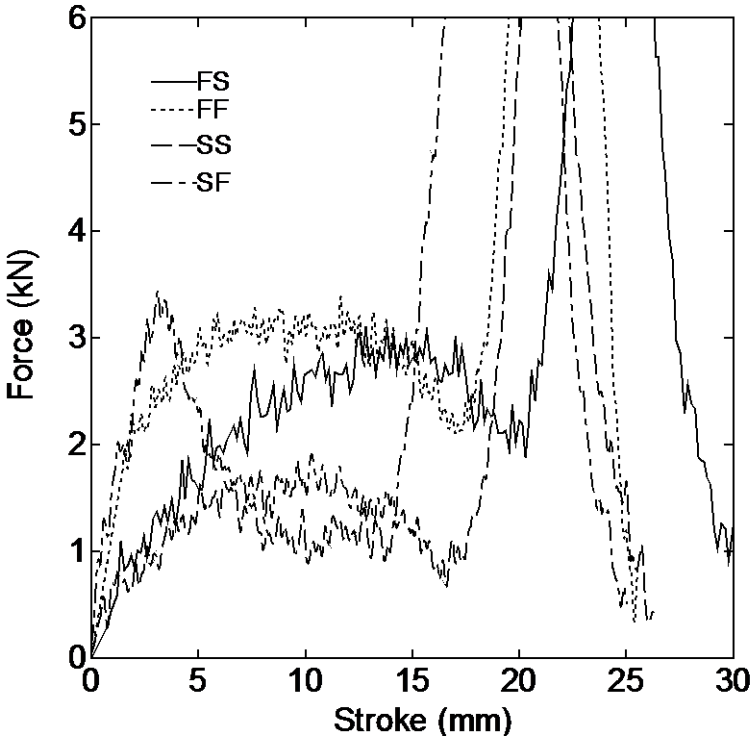

(b) Quasi-static test

Fig. 3.6.Force curves for flat top and hemispherical top shells of aluminium alloy.

3.4 Energy performance evaluation

The consumed energy in indentation is recognized as an index of energy absorption performance. Generally, deformation for energy absorption requires some space. The admissible space is usually considered to be the inner space of the shell. Hence, it may be appropriate to calculate the consumed energy in the travel length of the indentor equal to the shell height of 10 mm. The consumed energy E_C is defined in the form:

$$E_C = \int_0^{S_h} F(x)dx \tag{2.2}$$

where F is the indentation force and S_h is the shell height.

Fig. 3.7 summarises the absorbed energy for SPCE under various experimental conditions. The absorbed energy in impact deformation is greater than that in quasi-static one for all cases. The effect of sheet thickness is most prominent in the test with FF deformation condition. On the other hand, the energy increases almost linearly in other quasi-static tests, and this is possibly true also in impact test.

Further, indentation with 10 mm diameter indentor was carried out to study the evaluate the influence of indentor shape and size on the energy absorption performance. It was compared with the results obtained when the 30 mm diameter indentor was applied.

Energy absorption performance for the 10 mm indentation stroke was also evaluated using eq. (2.2), and exhibited in Fig. 3.8. Energy absorption performance for the flat headed shell is generally higher than that for hemispherical one.When comparing the energy absorption performance under impact for the 10 mm diameter indentor with the 30 mm one, the energy absorption performance of 10 mm indentor is around 20 % larger. The reason was such that the concentrated indentation force by the indentor caused severe bending to the shell's wall increasing the load to a higher level within the fracture limit of the shell height. On the other hand, the energy absorption performance under quasi-static condition for the 10mm indentor were only larger in the case of FS. This is attributed to that the shell fractures before the stroke equal to the shell height. This phenomenon implies that the ductility of the material becomes larger under high strain-rate plastic deformation.

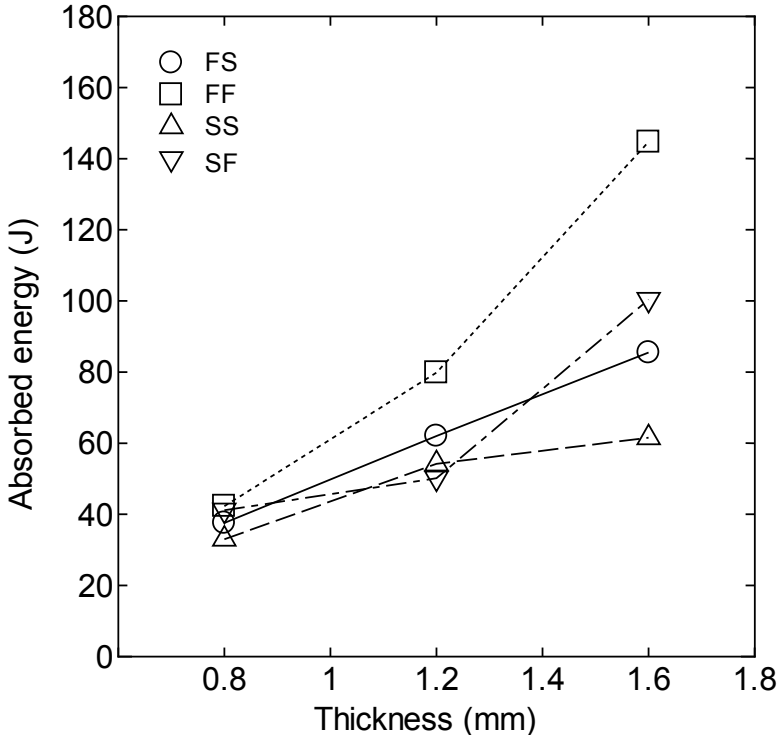

(a) Impact test

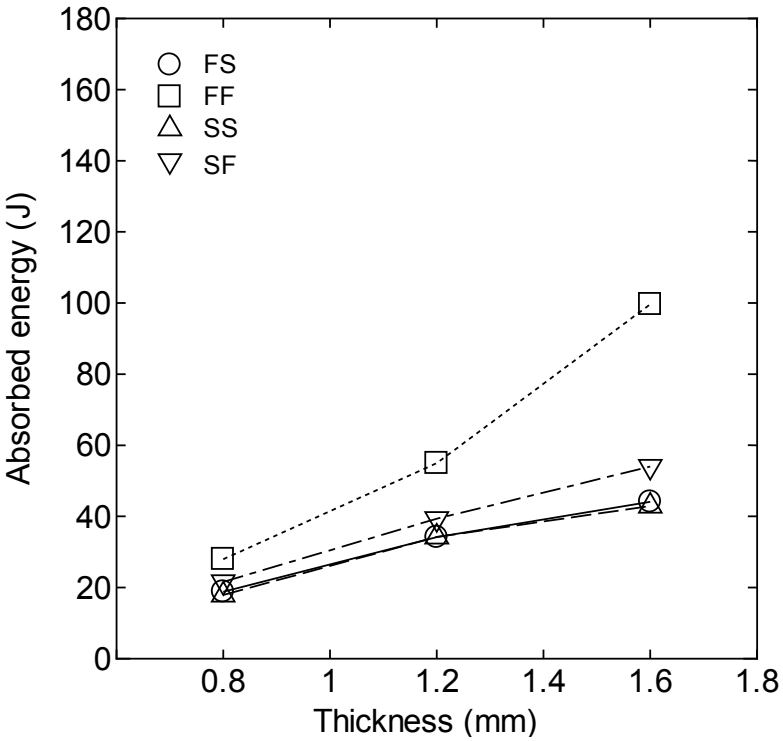

(b) Quasi-static test.

Fig. 3.7. Absorbed energy of SPCE in indentation stroke equal to shell height

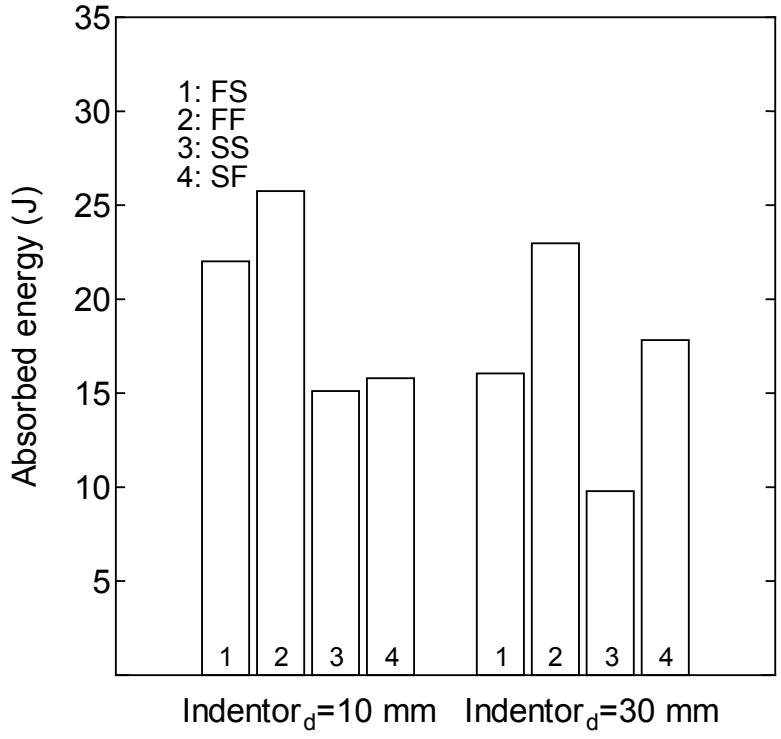

(a) Impact test

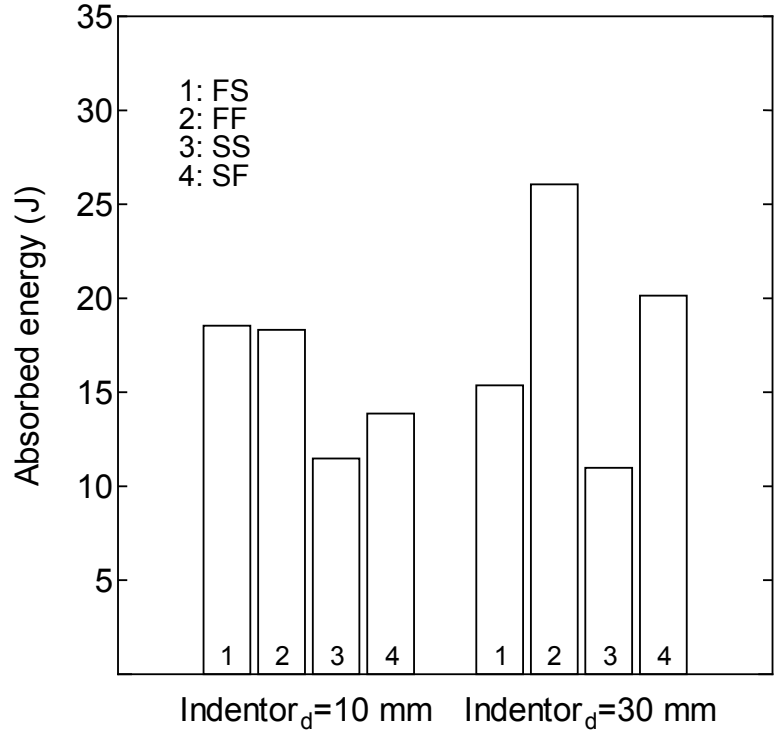

(b) Quasi-static test

Fig.3.8 Comparison of the absorbed energy in 10 mm indentation stroke

The energy absorbing performance was evaluated from the viewpoint of the weight saving design.The absorbed energy per unit mass E/m (J/g) is summarised in Fig. 3.9. The data obtained for the aluminium alloy A5052-H34 is also described for reference, because the thickness of aluminium alloy is 1 mm. The effect of sheet thickness on the energy absorption performance is definitely positive only for FF deformation condition in the case of SPCE. The effect is small or not clear for other deformation conditions. In the range of the present experiments, A5052-H34 and SPCE have comparable performance in energy absorption under impact, due to that the positive strain-rate effect becomes very remarkable in the present study, where the loading direction is reversed to that in the forming process.

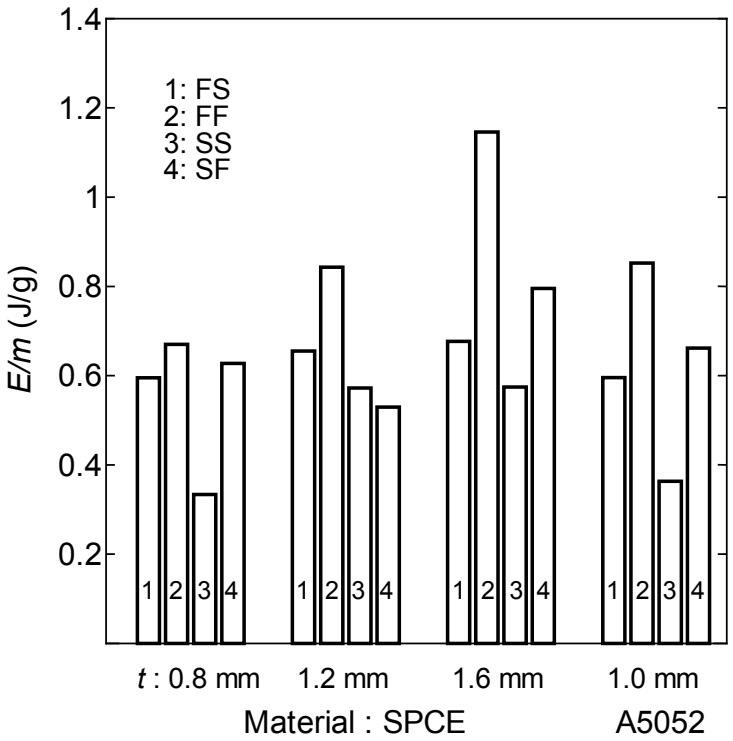

Fig. 3.9. Energy absorption performance considering mass of shell.

3.5 Conclusions

The press formed flat top or hemispherical shell was indented using flat or round headed indentor. Mild steel SPCE or aluminum alloy aluminum alloy A5052 shells were tested under impact or quasi-static deformation condition. The main conclusions are as follows:

Several characteristic force variations appeared. Almost flat indentation force is available in the combination of hemispherical shell and round headed indentor.The in-plane compressive stress field in the material induces the increase in indentation force, which increases the energy absorption capacity.

The force in impact test of SPCE was approximately 1.5 times higher than that in quasi-static test. The experimental resultobtained here implies that the strain-rate effect on the stress tends to be enhanced if the loading direction alters. On the other, aluminium alloy did not show the tendency.

Aluminum alloy A5052-H34 and mild steel SPCE have comparable performance in energy absorption under impact in the range of the present experiments. The positive strain-rate effect of SPCE under the reverse in loading direction may improve the performance.

When comparing the energy absorption performance under impact for the 10 mm diameter indentor with the 30 mm one, the energy absorption performance of 10 mm indentor is around 20 % larger. The reason was such that the concentrated indentation force by the indentor caused severe bending to the shell's wall increasing the load to a higher level within the fracture limit of the shell height.

Chapter 4: General Conclusions

This study is focusing on the energy absorbing performance for simple structures such as press-formed axisymetric shell. The test materials are mild steel sheet SPCE with 0.8, 1.2 or 1.6 mm thickness and aluminum alloy sheet A5052-H34 with 1 mm thickness. The shapes of the press formed shell are flat top and hemispherical. The material was aluminum alloy A5052-H34 sheet. Indentation was conducted using flat or hemispherical headed indentor. Shells are formed from a circular blank with 80 mm diameter using a hydraulic deep-drawing testing apparatus. The formed height is 10 mm. Impact energy absorption performance is investigated. The mass of the drop hammer indentor is 15 kg. The initial impact velocity is set to 5.0 m/s for SPCE and 3.4 m/s for A5052. Quasi-static test with 0.1 mm/s indentation speed was also carried out using a hydraulic press. And both impact and quasi-static test deformation behavior is investigated. Numerical simulation was also carried out by the dynamic explicit finite element method using aluminum alloy, A5052-H34 as test material model in order to present appropriate numerical model to achieve accurate prediction.

The study's main objective is to obtain the basic information in energy absorbing deformation behavior for constructing guideline to optimize the design of the collapsible components, e.g., in automobile and train bodies, building and structures.

In chapter 2, flat top and hemispherical aluminum alloy A5052 shells fabricated by the press forming were deformed by the flat or hemispherical headed indentor. Deformation patterns and characteristic of the indentation force were investigated. Energy absorption performance in indentation deformation of the shells was estimated for indentation stroke corresponding to the shell height. Numerical simulation was also carried out. The energy absorbing performance of the shell was greater in the case of flat headed indentor than in the case of hemispherical one. Axisymmetric plastic buckling deformation under in-plane axisymmetric compressive stress field was found very effective for the increase of the resistance to collapse. When the hemispherical shell was deformed by similar shaped indentor, less force variation was achieved due to the appropriately generated mobile plastic hinge. The deformation patterns obtained in experiment were well simulated by the finite element calculation. The accuracy in prediction of indentation force was improved by introducing the kinematic hardening plasticity in the material constitutive model, on the other hand, the force was overestimated when isotropic plasticity was applied. Bauschinger effect is one of the considerations in designing the press formed parts used as energy absorbing component.

In chapter 3, the press formed flat top or hemispherical shell was indented using flat or round headed indentor. Mild steel SPCE or aluminum alloy A5052 shells were tested under impact or quasi-static deformation condition. The main conclusions are as follows; Several characteristic force variations appeared. Almost flat indentation force is available in the combination of hemispherical shell and round headed indentor. The in-plane compressive stress field in the material induces the increase in indentation force, which increases the energy absorption capacity. The force in impact test of SPCE was approximately 1.5 times higher than that in quasi-static test. The experimental result obtained here implies that the strain-rate

effect on the stress tends to be enhanced if the loading direction alters. On the other, aluminium alloy did not show the tendency. Aluminum alloy A5052-H34 and mild steel SPCE have comparable performance in energy absorption under impact in the range of the present experiments. The positive strain-rate effect of SPCE under the reverse in loading direction may improve the performance. When comparing the energy absorption performance under impact for the 10 mm diameter indentor with the 30 mm one, the energy absorption performance of 10 mm indentor is around 20 % larger. The reason was such that the concentrated indentation force by the indentor caused severe bending to the shell's wall increasing the load to a higher level within the fracture limit of the shell height.

In summary, several useful characteristics were recognized for the design of press-formed shell parts considering energy absorption performance.

- Shell or indentor with more corners has better energy absorption performance. Especially, higher in-plane compressive stress field in the shell enables us to obtain much larger energy absorption performance per unit mass.
- If we control the mobile plastic hinges in the deforming shell properly, almost flat force response can be obtained.
- Strain-rate of aluminum alloy was found small. However, ductility was improved in high strain-rate deformation.
- Mild steel exhibits higher strain-rate effect when the shell deforms under inverse loading. The strain-rate effect was more enhanced compared with the conventional tensile test.

References

[1] Alghamdi, A.. Collapsible impact energy absorbers: an overview. Thin-Walled Structures, Vol.39, No.2 (2001), pp.189–213.

[2] Alghamdi, A.. Reinversion of aluminium frusta, Thin-Walled Structures, Vol. 40 (2002), pp.1037-1049.

[3] Olabi, A., Morris, E., Hashmi, M.. Metallic tube type energy absorbers: A synopsis. Thin-Walled Structures, Vol. 45 (2007), pp.706-726.

[4] El-Sobky, H., Singace, A.A.. An experiment on elastically compressed frusta. Thin-Walled Structures, Vol. 33 (1999), pp.231-244.

[5] Mohamed Sheriff, N., Gupta,N.K.. Optimization of thin conical frusta for impact energy absorption. Thin-Walled Structures, Vol. 46 (2008), pp.653-666.

[6] Niknejad,A., Tavassolimanesh, A.. Axial compression of the empty capped-end frusta during the inversion progress. Materials and Design, Vol. 49 (2013), pp.65-75.

[7] Mamalis, A.G., Manolakos, D.E. et al.. Extensible plastic collapse of thin-wall frusta as energy absorbers. International Journal of Mechanical Science, Vol. 28, No. 4 (1986), pp.219-229.

[8] Bisagni, C.. Crashworthiness of helicopter subfloor structures. International Journal of Impact Engineering, Vol. 27 (2002), pp.1067-1082.

[9] Pickett, A.K., Pyttel, T., Payen, F., Lauro, F., Petrinic, N., Werner, H., and Christlein, J.. Failure prediction for advanced crashworthiness of transportation vehicles. International Journal of Impact Engineering, Vol. 30, No. 7 (2004), pp.853-872.

[10] Yamashita, M., Gotoh, M., Sawairi, Y.. Axial crush of hollow cylindrical structures with various polygonal cross-sections: Numerical simulation and experiment. Journal of Materials Processing Technology, Vol. 140 (2003), pp.59-64.

[11] Jones, N.. Energy-absorbing effectiveness factor. International Journal of Impact Engineering, Vol. 37 (2010), pp.754-765.

[12] Jones, N.. Dynamic energy absorption and perforation of ductile structures. International Journal of Pressure Vessels and Piping, Vol. 87 (2010), pp.482-492.

[13] Kim, D-K, Lee S.. Impact energy absorption of 6061 aluminum extruded tubes with different cross-sectional shapes. Material and Design, Vol. 20 (1999), pp.41-9

[14] Abramowicz, W. and Norman, J.. Dynamic progressive buckling of circular and square tubes. International Journal of Impact Engineering, Vol.4, no.4 (1986), pp.243-270.

[15] Yamashita, M., Kenmotsu, H., Hattori, T.. Dynamic axial compression of aluminum hollow tubes with hat cross-section and buckling initiator using inertia force during impact. Thin-Walled Structures, Vol. 50 (2012), pp.37-44.

[16] Yamashita, M., Kenmotsu, H., and Hattori, T.. Dynamic crush behavior of adhesive-bonded aluminum tubular structure - Experiment and numerical simulation. Thin-Walled Structures, Vol.69 (2013), pp.45-53.

[17] White, M.D., Jones, N.. Experimental quasi-static axial crushing of top-hat and double-hat thin-walled sections. International Journal of Mechanical Science, Vol. 41 (1999), pp.179-208.
[18] Corbett, G.G., Reid, S.R., Al-Hassani, S.T.S.. Static and dynamic penetration of steel tubes by hemispherically nosed punches. International Journal of Impact Engineering, Vol. 9, No.2 (1990), pp.165-190.
[19] Zupana, M., Chen, C., Fleck, N.. The plastic collapse and energy absorption capacity of egg-box panels. International Journal of Mechanical Sciences, Vol. 45 (2003), pp.851-871
[20] Deshpande, V.S., Fleck, N.A.. Energy absorption of an egg-box material. Journal of the Mechanics and Physics of Solids, Vol. 51 (2003), pp.187-208.
[21] Gupta N.K., Prasad G.L. et al.. Axial compression of metallic spherical shells between rigid plates. Thin-Walled Structures, Vol. 34, No.1 (1999), pp.21-41.
[22] Gupta N.K., Ventakesh. Experimental and numerical studies of dynamic axial compression of thin walled spherical shells. International Journal of Impact Engineering, Vol. 30, Nos.8-9 (2004), pp.1225-1240.
[23] Gupta P.K., Gupta N.K.. A study of axial compression of metallic hemispherical domes. Journal of Materials Processing Technology, Vol. 209, No.4 (2009), pp.2175-2179.
[24] Shariati, M., Allahbakhsh, H.. Numerical and experimental investigations on the buckling of steel semi-spherical shells under various loadings. Thin-Walled Structures, Vol. 48 (2010), pp.620-628.
[25] Dong,X.L., Gao, Z.Y., Yu,T.X.. Dynamic crushing of thin-walled spheres: An experimental study, International Journal of Impact Engineering, Vol. 35 (2008), pp.717-726.
[26] Yamashita, M., Gotoh, M.. Impact behaviour of honeycomb structures with various cell specifications – numerical simulation and experiment. International Journal of Impact Engineering, Vol. 32 (2005), pp.618-630.
[27] E. Siebel. Niederhalterdruck beim tiefziehen. Stahl und Eisen, Vol. 74 (1954), pp.155-58.
[28] Yamashita, M., Hattori, T. and Nishimura, N.. Numerical Simulation of Sheet Metal Drawing by Maslennikov's Technique. Journal of Materials Processing Technology, Vol.187-188 (2007), pp.192-196.
[29] Yamashita, M., Hattori, T., Yamada, K. and Nishimura, N.. Frictional Effect on deformation behavior in incremental sheet forming. Steel Research International, Vol.81, No.9 (2010), pp.926-29.
[30] Halliquist, J.O.. Dyna3D Theoretical manual (1989).
[31] Tamura, S., Sumikawa, S., Uemori, T., Hamasaki, H. and Yoshida, F.. Experimental observation of elasto-plasticity behavior of type 5000 and 6000 aluminum alloy sheets. Materials Transactions, Vol.52, No.5 (2011), pp.868-875.
[32] Updike DP, Kalnins A.. Axisymmetric behavior of an elastic spherical shell compressed between rigid plates. ASME J Appl Mech, Vol. 92 (1970), pp.635-40.
[33] Updike DP, Kalnins A.. Axisymmetric post-buckling and non-symmetric buckling of a spherical shell compressed between rigid plates. ASME J Appl Mech, Vol. 94 (1972), pp.172-8.

[34] Yamashita, M., Zubair Bin Khalil. Deformation behavior of press formed shell by indentation and its numerical simulation. Hindawi Publishing, Journal of Engineering, Vol. 2015 (2015), Article ID 453931.
[35] Zubair Bin Khalil, Yamashita, M., Kuno, Y., Hattori, T.. Energy absorption performance of press-formed shell. Procedia Engineering, Vol. 81 (2014), pp. 951-956.